DR FENG WANG (Orcid ID : 0000-0001-7085-3816)

DR HONGTAO ZHONG (Orcid ID : 0000-0003-0674-0010)

PROF. HANS LAMBERS (Orcid ID : 0000-0002-4118-2272)

Article type : Regular Manuscript

Edaphic niche characterization of four Proteaceae reveals unique calcicole physiology linked to hyper-endemism of *Grevillea thelemanniana*

Jingwen Gao[1,2,†], Feng Wang[1,2,†], Kosala Ranathunge[1,†], André J. Arruda[1], Gregory R. Cawthray[1], Peta L. Clode[1,3], Xinhua He[4], Matthias Leopold[5], Ute Roessner[6], Thusitha Rupasinghe[6], Hongtao Zhong[1], Hans Lambers[1,*]

[1]School of Biological Sciences, University of Western Australia, Crawley, Perth, WA 6009, Australia.

[2]Environmental Resources and Soil Fertilizer Institute, Zhejiang Academy of Agricultural Sciences, Hangzhou, 310021, P. R. China.

[3]Centre for Microscopy, Characterisation and Analysis, University of Western Australia, Crawley, Perth, WA 6009, Australia.

[4]Center of Excellence for Soil Biology, College of Resources and Environment, Southwest University, Beibei, Chongqing, 400715, P. R. China.

[5]UWA School of Agriculture and Environment, University of Western Australia, Crawley, Perth, WA 6009, Australia.

[6]School of BioSciences, The University of Melbourne, Parkville, Melbourne, VIC 3010, Australia.

†These authors contributed equally.

*Author for correspondence: Hans Lambers

Email: hans.lambers@uwa.edu.au

Tel.: +61 8 6488 7381

Received: *20 April 2020*

Accepted: *15 July 2020*

Jingwen Gao (ORCID ID: https://orcid.org/0000-0002-1711-5811)

Feng Wang (ORCID ID: https://orcid.org/0000-0002-1788-8603)

Kosala Ranathunge (ORCID ID: https://orcid.org/0000-0003-2826-9936)

André J. Arruda (ORCID ID: https://orcid.org/0000-0001-8894-2585)

Gregory R. Cawthray (ORCID ID: https://orcid.org/0000-0003-1150-6675)

Peta L. Clode (ORCID ID: https://orcid.org/0000-0002-5188-4737)

Xinhua He (ORCID ID: https://orcid.org/0000-0002-5570-3454)

Matthias Leopold (ORCID ID: https://orcid.org/0000-0003-0716-0093)

Ute Roessner (ORCID ID: https://orcid.org/0000-0002-6482-2615)

Thusitha Rupasinghe (ORCID ID: https://orcid.org/0000-0001-7229-2469)

Hongtao Zhong (ORCID ID: https://orcid.org/0000-0003-0674-0010)

Hans Lambers (ORCID ID: https://orcid.org/0000-0002-4118-2272)

Summary

- Endemism and rarity have intrigued scientists for a long time. We focused on a rare endemic and critically-endangered species in a global biodiversity hotspot, *Grevillea thelemanniana* (Proteaceae).

- We carried out plant and soil analyses of four Proteaceae, including *G. thelemanniana*, and combined these with glasshouse studies. The analyses related to hydrology and plant water relations as well as soil nutrient concentrations and plant nutrition, with an emphasis on sodium (Na) and calcium (Ca).
- The local hydrology and matching plant traits related to water relations partially accounted for the distribution of the four Proteaceae. What determined the rarity of *G. thelemanniana*, however, was its accumulation of Ca. Despite much higher total Ca concentrations in the leaves of the rare *G. thelemanniana* than in the common Proteaceae, very few Ca crystals were detected in epidermal or mesophyll cells. Instead of crystals, *G. thelemanniana* epidermal cell vacuoles contained exceptionally high concentrations of non-crystalline Ca. Calcium ameliorated the negative effects of Na of the very salt-sensitive *G. thelemanniana*. Most importantly, *G. thelemanniana* required high levels of Ca to balance a massively accumulated feeding-deterrent carboxylate, *trans*-aconitate.
- This is the first example of a calcicole species accumulating and using Ca to balance accumulation of an antimetabolite.

Key words: Antimetabolite, calcicole, calcium, endemism, *Grevillea thelemanniana*, rarity, *trans*-aconitate, sodium exclusion

Introduction

Endemism and rarity have intrigued scientists for a very long time, as evidenced by Darwin's and Hooker's observations on the Galapagos flora (Darwin, 1845; Hooker, 1847; Kohn *et al.*, 2005). For most endemic species, we do not know which key adaptations enable them to flourish in their own specific environments, or how these adaptations prevent establishment or survival in neighbouring communities. Many rare plants are associated with environments that have distinctive edaphic characteristics, for example gypsum (Salmerón-Sánchez *et al.*, 2014; Escudero

et al., 2015), serpentine soils (Whittaker, 1954; Kruckeberg & Rabinowitz, 1985), limestone (Lee, 1998; Bothe, 2015) or other calcium-rich soils (Tansley, 1917; de Souza *et al.*, 2020), and soils enriched in metals (Brooks, 1998; Baker *et al.*, 2010). Shallow-soil endemics within the genus *Hakea* (Proteaceae) exhibit crack-exploring root traits that are advantageous in their own environments, but exclude them from adjacent habitats (Poot *et al.*, 2008; Poot & Lambers, 2008).

Grevillea thelemanniana Endl. (spider net grevillea; Proteaceae) is a critically-endangered shrub species found only in fragmented habitats southeast of Perth, Western Australia (Tauss *et al.*, 2019), in a global biodiversity hotspot (Myers *et al.*, 2000; Lambers, 2014). This species is part of a complex comprising 16 species and four subspecies, endemic to Western Australia, and belongs to a group with high conservation importance (Hevroy *et al.*, 2013). Our aim was to characterise the natural seasonal wetland habitat and the physiological traits of *G. thelemanniana* that possibly account for its rarity and endemism, comparing it with a co-occurring, but more widespread, species in the same family, *Banksia telmatiaea* A.S. George (swamp fox banksia). We also compared both with *Banksia attenuata* R.Br. (slender banksia) and *Banksia menziesii* R.Br. (firewood banksia), which grow near these two species, but in a much drier habitat.

Based on preliminary observations and the general belief that *G. thelemanniana* is associated with winter-wet low-lying flats and limestone, we studied specific aspects of plant water relations, including the stable isotope composition of water in soil and stem xylem, and mineral nutrition. Our focus was on calcium (Ca), to which most Proteaceae are very sensitive (Hayes *et al.*, 2019a; 2019b), phosphorus (P), which Proteaceae from P-impoverished habitats tend to both acquire and use extremely efficiently (Lambers *et al.*, 2015), and sodium (Na), which is present low in the profile in most soils in south-western Australia (Hatton *et al.*, 2003).We used elemental X-ray mapping to determine leaf cell-specific nutrient concentrations (Hayes *et al.*, 2018). Based on our results on plants growing in their natural habitat and in nutrient solutions in the glasshouse, we reveal unique traits of *G. thelemanniana* that underpin its rarity and endemism.

Excess Ca, associated with the putative limestone in its natural habitat, might precipitate as oxalate (McLaughlin & Wimmer, 1999) or sulfate crystals (He *et al.*, 2012) in cells, reducing its availability. Hence, we explored in which leaf cells and in which form Ca might accumulate in leaves of the calcicole and calcifuge Proteaceae.

Materials and Methods

Study area and species selection

We chose Alison Baird Reserve, one of very few locations where declared rare flora species and critically endangered *G. thelemanniana* co-exists naturally with the three other *Banksia* species studied here (Tauss *et al.*, 2019). It is a 34.6-ha flora reserve located southeast of Perth in south-western Australia (Fig. 1).

We selected four species of Proteaceae (*Grevillea thelemanniana*, *Banksia telmatiaea*, *Banksia attenuata* and *Banksia menziesii*) occurring naturally in Alison Baird Reserve, one of very few locations where, declared rare flora and critically-endangered *G. thelemanniana* occurs naturally (Tauss *et al.*, 2019). Salient traits of the four species are shown in Table S1. Alison Baird Reserve is a 34.6-ha flora reserve located 20 km southeast of Perth in south-western Australia (Fig. 1). The reserve lies in a region of poorly-drained flats on the Swan coastal plain at the foot of the Darling Scarp, from where sediments were imported and deposited into the reserve over millions of years (Lane & Evans, 2019). The clay flats have a shallow cover of sand, and are waterlogged in winter and dry in summer (Tauss *et al.*, 2019). The site is distinctive within the general area of the swampy flats, which are crossed diagonally by two ancient north-south Bassendean sand dunes, the larger eastern one rising up to 5-6 m above the flat, while the smaller western one is less than 2 m (Tauss *et al.*, 2019). Both ridges rise steeply on the western side with a long, gradual slope to the east (Tauss *et al.*, 2019). This reserve has a Mediterranean climate, with a pronounced dry period for about 5-6 months of the year, and cool wet winters (Gentilli, 1972).

Soil and leaf sample collection in the field

Soil samples from different horizons at 0-5 m depth were taken for analysis in August (winter) 2018 from three different sites; the east and west with intermittent waterlogging in the rainy winter and dry in the summer where *G. thelemanniana* and *B. telmatiaea* coexist, and the sand dune where *B. attenuata* and *B. menziesii* occur together (Fig. 1). Samples were also collected in March (summer) 2018 and August (winter) 2018 for the analysis of δ^2H_{liq} and $\delta^{18}O_{liq}$ in soil water.

Leaf samples of all species were collected in the field for nutrient and cell-specific element analysis in August (winter) 2018. Fully-expanded leaves were selected from four plants of each species, and one healthy stem from each plant was cut and immediately placed in a zip lock plastic bag for xylem sap collection. The freshly collected samples were placed in a cool box with ice and transported to the laboratory.

Soil electrical conductivity (EC) was measured using an EC meter in 1:5 soil-to-DI water. Soil total organic carbon (TOC) content was estimated by dividing the total organic matter (measured as loss on ignition) with a conversion factor of 1.72 (Rayment & Lyons, 2011). Total nitrogen (TN) was measured by the combustion method via a Leco analyser (FP628, St. Joseph, MI, USA).

Plant growth in hydroponic culture

Grevillea thelemanniana plants were propagated from stem cuttings by Apace Nursery, Fremantle, Australia. *Banksia telmatiaea* plants were grown from seeds collected in the Alison Baird Reserve. Seeds were sterilised with 1% (v/v) bleach solution for 20 seconds, followed by 70% (v/v) ethanol for another 20 seconds, shaking continuously, then rinsed thoroughly in DI water. Seeds were germinated on moist filter papers (15 °C, 12 h: 12 h, light: dark). When the cotyledon length reached 1 cm, seedlings were transferred to steam-sterilized silica sand, and watered twice a day with deionised water. Plants were grown in a temperature-controlled glasshouse with a mean temperature of 21 °C. Six weeks later, healthy plants were transferred to 4-L containers with continuously aerated nutrient solution. The composition of the solution was as described previously (Hayes *et al.*, 2019b). Each pot had one plant and was maintained at 18 °C by placing

pots in a root-cooling tank.

Growth with different concentrations of sodium (Na) combined with calcium (Ca)

A hydroponic experiment was conducted between October and December 2018. Uniform *G. thelemanniana* and *B. telmatiaea* plants were transferred to 4 L containers with continuously aerated nutrient solution. During acclimation in the glasshouse, the strength of the nutrient solution was increased gradually from 25% to 100% (pH = 5.8) as previously described (Hayes *et al.*, 2019b). During this period, Na and Ca were supplied at 0 and 0.1 mM, respectively. Once plants were established in hydroponics, they were supplied with different Na (0, 5 or 10 mM; supplied as NaCl) and Ca (0.1 or 1.2 mM; supplied as $CaCl_2$) concentrations and grown on for further 4 weeks. The nutrient solution was changed three times per week.

Growth with different concentrations of Ca

Another set of plants were grown in aerated hydroponics between September and December 2018. The growing conditions and nutrient concentrations were the same as mentioned above. Calcium treatments were based on previous experiments investigating calcifuge/calcicole species (Jefferies & Willis, 1964; Hayes *et al.*, 2019b). In this experiment, plants were supplemented with three different Ca concentrations (0, 0.6 or 6.0 mM; supplied as $CaCl_2$) for 4 weeks without Na. Although it is difficult to directly compare hydroponic nutrient concentrations with those in soil, use of hydroponic experiments does allow for a highly controlled investigation of the impact of specific nutrient on plant growth and health. All nutrient solutions were replenished three times per week. Despite no additional Ca being added under the 0 mM Ca treatment, there would be a very low background level of Ca in the deionised water.

Soil and leaf nutrient analyses

Particle size distribution of the soil samples was measured through laser diffraction (Ryżak & Bieganowski, 2011), using a Mastersizer 2000 with 200G wet dispersion accessory (Malvern Panalytical, UK). Soil samples were sieved (<2 mm), homogenised and air-dried before chemical analyses. Soil pH was measured using a pH meter in a 1:5 soil-to-solution in 0.01 M $CaCl_2$

(Rayment & Lyons, 2011). Soil exchangeable cations were determined by $BaCl_2$ (0.1 M) extraction and inductively coupled plasma optical emission spectrometry (ICP-OES) Model 5300DV (Perkin Elmer, Shelton, CT, USA) (Rayment & Higginson, 1992). To determine soil available P, samples were shaken for 16 h in 1:200 soil-to-solution using (0.5 M $NaHCO_3$, pH 8.5) as extraction solution (Rayment & Lyons, 2011).

Aliquots of 100 mg of freeze-dried ground leaf samples and two reference samples were acid-digested using 4 mL of concentrated HNO_3: $HClO_4$ (3:1) and then DI water was added to end up with a volume of 10 mL. The total P concentration was determined colorimetrically using the malachite green method (Motomizu *et al.*, 1983). Other elements were determined by ICP-OES Model 5300DV (Perkin Elmer, Shelton, CT, USA). Reference samples were included after every 20 samples during analysis.

Water potential (ψ_w), percent loss of hydraulic conductivity (PLC) of stems and leaf osmotic pressure (π)

The water potential of plant tissues of all species was measured using a PMS 1000 pressure chamber (PMS, Corvallis, OR, USA). A separate set of branches were cut into 3-cm long segments under water, and connected to a modified Sperry apparatus (Sperry *et al.*, 1988) to measure the PLC (Canham *et al.*, 2009; Zhang *et al.*, 2018). To measure leaf osmotic concentration, leaves were crushed, the sap was collected and diluted 10 times with distilled water, and measured with a Kanuer K-7200S semi-micro freezing point osmometer (Berlin, Germany). The resulting concentration in mOsmol kg^{-1} was converted to osmotic pressure using the Van't Hoff equation: $\pi = MiRT$ with M = concentration in molarity, i = Van`t Hoff factor, R = ideal gas constant, T = absolute temperature (K).

δ^2H_{liq} and $\delta^{18}O_{liq}$ of stem xylem sap and soil water

Xylem sap of the stems was collected by applying pneumatic pressure using a PMS 1000 pressure chamber (PMS, Corvallis, OR, USA). Soil water was extracted by distillation, and cryogenic collection in a Pyrex glass U-trap with alcohol lamp for heat on the distillation side of the trap and

ice cooling on the collection side until no additional water was recoverable (verified by no further condensation inside the distillation apparatus; extraction time >100 min). Extracted water samples were measured for δ^2H_{liq} and $\delta^{18}O_{liq}$ values using a Picarro L-2130i Water Isotope Analyser (Picarro Inc., Santa Clara, CA, USA) (Good *et al.*, 2014), and the data were screened with Chem Correct software to identify potential artifacts associated with spectroscopic interferences. Based on results from standard water samples analysed concurrently, analytical precision for these liquid water analyses was ± 0.3‰ for δ^2H and ± 0.03‰ for $\delta^{18}O$. Isotope values are reported in δ notation and liquid and vapour H_2O δ^2H and $\delta^{18}O$ values are referenced to the Vienna Standard Mean Ocean Water (VSMOW) (Coplen, 1994).

Leaf gas exchange and chlorophyll fluorescence measurements

Gas exchange and chlorophyll fluorescence measurements were conducted on the youngest fully-expanded leaves in the morning between 9:00 and 11:00 am with a LI6400XT portable photosynthesis system (Li-Cor 6400, Li-Cor Inc., Lincoln, Nebraska, USA). During measurements, leaf temperature was maintained at 25.0 ± 0.5°C, under a steady red and blue light source with a photosynthetic photon flux density of 800 μmol photons m^{-2} s^{-1}. The reference CO_2 concentration, vapour pressure and relative humidity were 400 μmol mol^{-1}, 1.1 ± 0.05 kPa and 55-65%, respectively.

Light-adjusted chlorophyll fluorescence was measured simultaneously with gas exchange measurements as mentioned above. The steady-state fluorescence (F_s) was measured under actinic light. A saturating light pulse (~8000 μmol photons m^{-2} s^{-1}) was applied for 0.7 s to obtain the maximum fluorescence (F_m'). After removing the actinic light and applying 3 s of far-red light, the minimal fluorescence of the light-adjusted state (F_o') was obtained. The minimum and maximum chlorophyll fluorescence (F_o and F_m) values were determined after full dark adjustment for at least 30 min. F_s, F_m' and F_o' were obtained as the same way mentioned above. The quantum efficiency of PSII (Φ_{PSII}) and maximum quantum efficiency of photosystem II (F_v/F_m) were calculated as previously described (Genty *et al.*, 1989).

Leaf carboxylate extraction and analysis

Field-collected leaves of *G. thelemanniana* and *B. telmatiaea* were immediately immersed in liquid N_2 and stored at –80 °C. The material was freeze-dried (VirTis Co., Gardiner, NY, USA) and ground in a ball-mill grinder using plastic vials and yttrium-stabilised zirconium ceramic beads. Approximately, 20 mg of freeze-dried, ground leaf tissues were weighed into Eppendorf tubes. Subsequently, 500 µL of 100% methanol containing 4% internal standard (from a stock solution containing 0.5 mg mL^{-1} $^{13}C_6$-sorbitol/valine) was added to the samples. The samples were then shaken 20 min at 30 °C in a thermomixer at 21,100 × g, and subsequently centrifuged for 10 min at 4 °C at 18,400 × g. The supernatants were transferred into new Eppendorf tubes, and 400 µL of MilliQ water was added into the tubes containing the pellet. The samples were vortex-mixed for 1 min, and centrifuged at 18,400 × g for 10 min at 4 °C. The supernatants were then transferred into the Eppendorf tube containing the original supernatant from the previous centrifugation. After the pooled samples were vortex-mixed for 30 s, 20 µL aliquots of the supernatants were transferred into glass vial inserts and dried in vacuo for Gas Chromatography–Triple Quadrupole Mass Spectrometry (GC–QqQ–MS) analysis. Samples were 50 times diluted before analysis.

Since GCMS did not allow for separation of *cis*- and *trans*-aconitate, we used a separate analysis. Ground samples of 20 mg were extracted with 1.5 mL of cold 5% (w/v) perchloric acid while being kept on ice at all times (Keerthisinghe *et al.*, 1998). Samples were centrifuged at 21,200 × g for 30 minutes at 4°C; the supernatant was removed and kept on ice while the pellet was extracted a second time with 1.5 mL of cold 5% (w/v) perchloric acid. After centrifugation, supernatants were combined, pH adjusted to 3 with K_2CO_3, and then analysed by High Performance Liquid Chromatography (HPLC) (Cawthray, 2003). Standards of *cis*- and *trans*-aconitate were taken through the extraction procedure to monitor the stability of each stereoisomer during the extraction process.

Microscopy

Mature fully-expanded leaves were collected, cut into 1 cm length segments and fixed in 2.5% glutaraldehyde + 1.6% paraformaldehyde in PBS. The fixed samples were dehydrated, critical

point-dried, mounted and coated with gold and then scanned at 10 kV using a scanning electron microscopy (SEM) system (Zeiss 55, Zeiss, Pleasanton, CA, USA). To visualise the presence and distribution of crystals, leaves that were chemically fixed in 2.5% glutaraldehyde + 1.6% paraformaldehyde in PBS were scanned using a Zeiss Versa 520 X-ray microscope at 80 kV and 7 W, with 2401 projections over the full 360° range. Magnifications and exposure times were optimised for each leaf sample to scan the entire width of the leaf and to produce ~10000 counts in a single exposure. Data were reconstructed and visualised using the instrument software. Data are presented as 2-D maximum intensity projection images to optimally display the location of biominerals within the leaf tissues.

For cell-specific element analyses, leaf segments were freshly excised, glued to an aluminium grooved pin, and rapidly plunge frozen into liquid N, thereby immediately immobilizing and preserving cellular ions (Hayes *et al.*, 2018). Transverse sections of frozen leaf segments were prepared by cryoplaning a flat surface using a cryomicrotome before being coated, without sublimation, with 20 nm Cr (Kotula *et al.*, 2019). Samples were analysed in a cryo-scanning electron microscope (Zeiss 55 Supra SEM, Zeiss, Pleasanton, CA, USA) fitted with a SDD EDS detector (Oxford Instruments) at –150°C, 15 kV, and a 2 nA beam current, in high current mode. Immediately prior to acquisition of each map, the instrument was calibrated and the beam current measured using a pure copper standard. Elemental maps were acquired at 512 pixel resolution, for >3000 frames with a dwell time of 10 μs per pixel. Drift correction and pulse-pile up correction were activated. Cellular analyses and element quantification were performed using AZtecEnergy software (Oxford Instruments) (Hayes *et al.*, 2018). Cells that were analysed comprised upper epidermis (UE), palisade mesophyll (PM), spongy mesophyll (SM), and lower epidermis (LE).

Statistical analyses

The effects of the treatments and species on the investigated morphological, physiological and biochemical parameters were analysed by a two-way analysis of variance (ANOVA) by Dunnett's multiple comparison test at $P < 0.05$ in Figs 2, 3, 4, 5a and 7c using SPSS statistical package

(SPSS Inc., Chicago, IL, USA). In Fig. 5b, correlations between plant dry weight, net photosynthetic rate (P_n), concentrations of leaf nitrogen ([N]), phosphorus ([P]) and calcium ([Ca]) were derived from a linear model. In Figs 7a and b, an unpaired student's t-test was used to compare carboxylate concentrations in leaves at $P < 0.05$.

Results

Plant water relations

The δ^2H_{liq} and $\delta^{18}O_{liq}$ values detected in the soil layers close to the surface were higher (less negative) than in the deeper layers (Fig. 2a, b). Both δ^2H_{liq} and $\delta^{18}O_{liq}$ values of all species were more negative in summer than in winter, and showed major differences among species, especially in summer (Fig. 2c, d). In winter, plants accessed ground water around 1.5 to 4.5 m below the soil surface, and in summer, they acquired water from deeper soil layers. More negative values of *B. menziesii* and *B. attenuata* on top of the sand dune indicate they accessed deep ground water, especially in summer. The values of water potential showed no significant difference among species in winter, but were much more negative in summer, especially in the wetland species, *G. thelemanniana* and *B. telmatiaea* (Fig. 2e). All species showed some water stress (~20% percent loss of conductivity (PLC) in the stem) in winter, but significantly more (~50% PLC) in summer (Fig. 2f).

Nitrogen, P, Ca and Na concentrations

The rare *G. thelemanniana* had a somewhat greater leaf [N], approximately 13-14% greater than that in *Banksia* species (Fig. 3a). *Grevillea thelemanniana* also had the highest leaf [P], approximately 26% greater than that in *Banksia* species (Fig. 3b), and accumulated Ca in its leaves, approximately 10-fold more than *Banksia* species (Fig. 3c). Conversely, it contained lower sodium concentration ([Na]), approximately 30-35% of that in the *Banksia* species (Fig. 3d).

Soil chemical properties in Alison Baird Reserve

The pH was generally very acid across all sites in the topsoil horizons (Table 1). The depth trend of soil pH showed a general increase with depth in all profiles, with the sharpest increase in the Bs2 horizon (4.3-5.0 m) on the dune.

The electrical conductivity (EC) and cation exchange capacity (CEC) in the topsoil horizons were lower than in the subsoil horizons, especially on the dune. In general, the CEC values were greater on eastern and western swampy sites than on the dune (Table 1) reflecting the differences in soil texture.

The concentrations of exchangeable calcium (ex-Ca) were greater in the B2 horizons (starting at 2.6 m at the eastern site and at 0.67 m at the western site) compared with the topsoil horizons (Table 1). Concentrations of exchangeable sodium (ex-Na), potassium (ex-K) and magnesium (ex-Mg) followed a similar trend. The sand dune profile which basically sits on top of the soil horizons of the western and eastern site, only showed slightly increased values of CEC and exchangeable cations at the base of the profile. In general, the soils in this area were extremely impoverished in N and P, with the exception of plant available P in the topsoil horizons of the eastern and western swampy sites.

At all sites, the percentage of total organic carbon (TOC) decreased with soil depth, with overall greater contents at the swampy eastern and western sites (Table 1). TOC values of the sand dune site reflected the soil horizons with higher values in the Ah horizon down to 30 cm. Deeper down the profile the eluviated E horizon showed no TOC but subsoil horizons provided a small amount of organic carbon most likely transported down through the E horizon.

The soil texture of all topsoils can be classified as sand. Subsoil texture was a loamy sand for the western and eastern profile but remained sandy for the dune profile (Table 1).

Table 1. Soil characteristics of different soil horizons at 0-5 m depth next to four Proteaceae species in Alison Baird Reserve, south-western Australia.

Eastern site (11 m asl)		***Chemical parameters***										***Physical parameters***		
Soil horizon	**Depth**	**pH**	**EC**	**CEC**	**ex- Al**	**ex- Ca**	**ex- K**	**ex- Mg**	**ex- Na**	**TN**	**TOC**	**P (col)**	**Sand**	**Silt**	**Clay**
	[m]	[$CaCl_2$]	[mS m^{-1}]	meq kg^{-1}	meq kg^{-1}	meq kg^{-1}	meq kg^{-1}	meq kg^{-1}	meq kg^{-1}	[%]	[%]	[mg kg^{-1}]	[%]	[%]	[%]
Ah	0-0.15	4.4	2.0	13.8	0.3	8.7	1.0	2.9	0.3	0.05	0.80	1.17	93.9	5.7	0.4
E	0.15-0.30	4.2	1.4	11.4	0.7	2.7	0.5	2.4	0.1	0.03	0.33	0.50	95.1	4.5	0.4
B2	0.30-2.60	3.9	4.5	39.2	9.2	4.2	0.9	15.4	4.8	0.02	0.18	0.10	89.7	8.9	1.4
B3	2.60-5.00	5.1	40.9	71.9	0.3	9.7	2.6	34.7	35.1	0.02	0.04	0.14	89.3	8.9	1.9
Western site (9 m asl)		***Chemical parameters***										***Physical parameters***		
Soil horizon	**Depth**	**pH**	**EC**	**CEC**	**ex- Al**	**ex- Ca**	**ex- K**	**ex- Mg**	**ex- Na**	**TN**	**TOC**	**P (col)**	**Sand**	**Silt**	**Clay**
	[m]	[$CaCl_2$]	[mS m^{-1}]	meq kg^{-1}	meq kg^{-1}	meq kg^{-1}	meq kg^{-1}	meq kg^{-1}	meq kg^{-1}	[%]	[%]	[mg kg^{-1}]	[%]	[%]	[%]
Ah	0-0.10	4.1	2.3	250.0	0.0	54.0	6.0	19.0	7.0	0.08	1.42	0.98	97.5	2.5	0.0
E	0.10-0.44	3.9	1.6	5.5	0.4	30.5	4.0	30.0	8.5	0.05	0.59	0.45	98.7	1.4	0.1
Bhs	0.42-0.67	4.3	6.5	340.0	0.4	125.0	7.0	137.5	73.5	0.08	1.40	0.53	92.1	7.4	0.5
B2	0.67-3.47	5.4	59.7	1234.0	0.0	262.8	47.6	669.4	763.6	0.04	0.40	0.21	82.9	14.7	2.4
B3	3.47-5.00	6.7	34.5	813.3	0.2	297.0	55.5	529.0	428.8	0.02	0.03	3.22	87.2	9.3	3.5

Sand dune (15 m asl)		*Chemical parameters*										*Physical parameters*		
Soil horizon	**Depth**	**pH**	**EC**	**CEC**	**ex- Al**	**ex- Ca**	**ex- K**	**ex- Mg**	**ex- Na**	**TN**	**TOC**	**P (col)**	**Sand**	**Silt**	**Clay**
	[m]	[$CaCl_2$]	[mS m^{-1}]	meq kg^{-1}	meq kg^{-1}	meq kg^{-1}	meq kg^{-1}	meq kg^{-1}	meq kg^{-1}	[%]	[%]	[mg kg^{-1}]	[%]	[%]	[%]
Ah	0-0.30	4.2	1.9	5.0	0.0	1.4	0.0	0.5	0.0	0.01	0.19	0.18	99.3	0.7	0.0
E	0.30-3.65	4.7	0.5	2.0	0.0	0.0	0.0	0.0	0.0	0.00	0.00	0.20	98.1	1.6	0.3
Bh	3.65-4.30	4.5	7.0	20.0	0.8	0.6	0.9	0.1	0.5	0.20	0.02	0.82	97.5	2.5	0.0
Bs	4.30-5.00	6.4	59.7	60.0	55.7	0.1	19.5	1.6	25.8	2.73	0.02	1.00	96.4	3.6	0.0

Absolute elevations of different sites are given in m asl (above sea level). EC: electrical conductivity; MS: magnetic susceptibility; CEC: cation exchange capacity; ex-Ca: exchangeable calcium concentration; ex-Na: exchangeable sodium concentration; TN: total nitrogen concentration; TOC: total organic carbon concentration; Colwell P: plant-available phosphorus (P) concentration; grav %: gravitational percentage; Ah: topsoil horizon rich in organic material; E: eluvial horizon; B1-3: number of subsoil horizon; Bh: subsoil horizon enriched with organic material; Bs: subsoil horizon enriched with sesquioxides (humosesquic). The world reference base for soils was used for soil classification (Schad *et al.*, 2014).

Effects of Ca on Na uptake in roots

Since we did not find water with a low Na concentration at greater depth (Table 1) from which *G. thelemanniana* takes up water (Fig. 1), it is highly likely that it excludes Na. To determine whether Ca plays a role in this putative Na exclusion in *G. thelemanniana* and *B. telmatiaea*, we grew plants of both species with different Na and Ca concentrations in aerated hydroponics in a glasshouse. When grown with as low as 0.1 mM Ca, biomass content of *G. thelemanniana* decreased with increasing Na concentration (Fig. 4a). However, when grown with 1.2 mM Ca, the 5 mM Na treatment decreased biomass of *G. thelemanniana* only by 31% compared with that at 0 mM Na, and this reduction was approximately 38% at 10 mM Na (Figs 4a, S1). In comparison, 10 mM Na did not significantly reduce the growth and biomass of *G. thelemanniana* compared with growth at 5 mM Na, when grown with 1.2 mM Ca (Fig. 4a). In contrast, *B. telmatiaea* exhibited Na insensitivity and did not show any correlation between biomass and Na or Ca treatments (Fig. 4a). For both *G. thelemanniana* and *B. telmatiaea*, foliar [Na] increased with increasing Na supply (Fig. 4b). The 1.2 mM Ca treatment significantly reduced foliar [Na] compared with the 0.1 mM Ca treatment for both species, presumably due to reducing Na uptake by roots, but the effect was more pronounced for *G. thelemanniana*.

The Na treatments increased leaf water content in *G. thelemanniana*, but not in *B. telmatiaea* (Fig. 4c). However, treatment with 1.2 mM Ca restored the leaf water content in *G. thelemanniana* to that at 0 mM Na (Fig. 4c). In both species, the leaf osmotic potential decreased (more negative) with increasing [Na], but this was more pronounced in *G. thelemanniana* (Fig. 4d). The 1.2 mM Ca treatment restored leaf osmotic potential of both species, specifically in *G. thelemanniana*. In contrast, a Ca treatment of 0.1 mM failed to restore leaf osmotic potential of both species under both Na treatments (Fig. 4d).

The net photosynthesis and transpiration rates decreased significantly with increasing [Na] in *G. thelemanniana*; however, the 1.2 mM Ca treatment remarkably restored net photosynthesis and transpiration rates compared with the low Ca treatment (Figs 4e, f). In contrast, *B. telmatiaea*

coped much better with Na treatments, and only 10 mM Na significantly reduced transpiration rates, but the 1.2 mM Ca treatment restored it (Fig. 4f).

The maximum quantum efficiency of photosystem II (F_v/F_m) and quantum efficiency of PSII (Φ_{PSII}) decreased with increasing [Na] only in *G. thelemanniana*, but the 1.2 mM Ca treatment successfully restored both (Figs 4g, h).

Effects of different Ca levels

The [Ca] in leaves, stems and roots increased with increasing Ca supply (Fig. 5a), but *G. thelemanniana* showed significantly higher leaf and root [Ca] than *B. telmatiaea,* whereas it was the opposite for stems (Fig. 5a). There was a strong positive correlation between leaf [Ca] and plant dry weight, net photosynthesis rate, and leaf [N] and [P], but not between leaf [Ca] and [P] in *G. thelemanniana* (Figs 5b; S2). The rare *G. thelemanniana* exhibited steeper slopes and pronounced correlations between leaf [Ca] and plant dry weight and net photosynthetic rate than *B. telmatiaea*.

Calcium crystals

Despite much higher [Ca] in *G. thelemanniana* leaves, we detected very few Ca crystals in any cells by X-ray micro-computed tomography (Fig. 6). The large amount of Ca in the leaves (Fig. 3c) is obviously not in the typical crystalline form. Conversely, in the species with much lower leaf [Ca], Ca crystals with typical druse morphologies were abundant in *B. telmatiaea* (located in mesophyll cells), *B. menziesii* (located in palisade mesophyll and spongy mesophyll cells) and *B. attenuata* (located in palisade mesophyll and spongy mesophyll cells). We also detected ovoid silica (Si)-based crystals in epidermis cells in *B. telmatiaea* and *B. attenuata* (Fig. S3), consistent with common phytoliths.

Accumulation of carboxylates and Ca ions

Grevillea thelemanniana accumulated large amounts of leaf carboxylates, especially aconitate, whose concentration was about 1100 times greater than that in *B. telmatiaea* (Fig. 7a). In *G. thelemanniana*, approximately 98% of aconitate was *trans*-aconitate (Fig. 7b), while in *B. telmatiaea*, approximately 89% of aconitate was *trans*-aconitate.

Calcium accumulated in specific cells of the leaves, and there was a significant variation in the patterns of Ca accumulation between species. Leaves of *G. thelemanniana* exhibited much higher [Ca] than *B. telmatiaea*, and a much greater amount accumulated in epidermal cells (EP), followed by spongy mesophyll (SM) cells (Figs 7c, d). In *B. telmatiaea*, Ca mostly accumulated in SM cells; however, this concentration was only 1/3 of that in SM of *G. thelemanniana*. Data for *B. menziesii* and *B. attenuata* have been published by Hayes et al. (Hayes *et al.*, 2018; Hayes *et al.*, 2019a).

Discussion

Grevillea thelemanniana (spider net *Grevillea*) is an endemic, critically endangered and threatened species with a very narrow distribution. Our analyses of edaphic characteristics in its natural habitat and its physiological traits have helped to provide a clear explanation for why it is rare and threatened. First, it requires access to water throughout the year, especially in the dry summer, and it shares this requirement with the co-occurring *B. telmatiaea*, swamp fox *Banksia* (this study). Therefore, *G. thelemanniana* and *B. telmatiaea* are restricted to winter-wet low-lying flats or swampy areas. Second, *G. thelemanniana* operates at approximately 30% greater P levels than most of the other Australian Proteaceae in south-western Australia, and this a typical trait for other *Grevillea* species (Wright *et al.*, 2004). This implies that most sandy soils supporting Proteaceae are too poor for *G. thelemanniana*, which prefers marginally richer soils lower in the landscape (Table 1). Most importantly, unlike most Proteaceae, *G. thelemanniana* requires greater amounts of Ca, but not because this is sequestered in crystals, as in other Proteaceae (Fig. 6), but to balance accumulation of a feeding-deterrent carboxylate, *trans*-aconitate in the leaves. This is the first

record of a calcicole species using Ca for this to balance an antimetabolite.

Water relations determine distribution of *G. thelemanniana* and *Banksia* species

Water availability is an important factor determining the distribution of plant species, and species with a high water demand and low hydraulic conductivity are restricted to habitats where plants can access water all year round (Canham *et al.*, 2009). In the present study, there was no significant difference in leaf water potential among four species in winter. However, leaf water potential in *G. thelemanniana* and *B. telmatiaea* decreased significantly in summer compared with that in winter. In contrast, this change was less in *B. menziesii* and *B. attenuata* (Fig. 2e). Lower leaf water potentials in *G. thelemanniana* and *B. telmatiaea*, which are spreading, lignotuberous shrubs, allowed them to access more water from the loam at depth, but a more negative water potential does not allow greater water access from sand (Pavlik, 1980), in which *B. menziesii* and *B. attenuata* grew. The latter two species are taller trees with deep roots systems, which had access to deep ground water. Besides, a lower water potential in drought conditions is related to less tight stomatal control and continuous transpirational water loss from plants which leads to partial loss of hydraulic conductivity because of xylem embolisms (Tyree & Sperry, 1989). As a result, there is a greater risk of loss of hydraulic conductivity in *G. thelemanniana* and *B. telmatiaea* in hot dry summers, when access to water is limited. However, there was no pronounced difference in percent loss of conductivity (PLC) among the four species, either in winter or in summer (Fig. 2f). As water isotopic composition does not change during water uptake from soil by roots and transport to shoots (Ehleringer & Dawson, 1992), analyses of hydrogen or oxygen isotopic composition in xylem sap and different soil layers allowed us to determine from which soil layers plants absorbed water. In the present study, *G. thelemanniana* and *B. telmatiaea* acquired water at a depth of 2-3 m in winter and 4-5 m in summer, while *B. menziesii* and *B. attenuata* took up water from a depth of 4-5 m in winter and even deeper in summer (Fig. 2a-d). These results indicate that *B. menziesii* and *B. attenuata* took up water from deeper layers than *G. thelemanniana* and *B. telmatiaea* did; thus, the latter species encountered a greater risk of xylem cavitation and loss of hydraulic conductivity under drought, resulting in their distribution in

low-lying wet areas.

Grevillea thelemanniana operates at higher leaf P levels than _Banksia_ species

During pedogenesis and ecosystem development, soil P availability declines, becoming the major nutrient limiting plant growth in ancient weathered soils (Walker & Syers, 1976; Peltzer *et al.*, 2010; Turner & Laliberté, 2015), such as those in south-western Australia (Lambers *et al.*, 2012). South-western Australian Proteaceae species have evolved with several traits to survive in severely P-impoverished soils (Lambers *et al.*, 2018). In the present study, leaf P concentration was significantly higher (approximately 30%) in *G. thelemanniana* than in the *Banksia* species (Fig. 3b), indicating that its growth demanded more P, which is common for *Grevillea* species (Wright *et al.*, 2004). Obviously, there was adequate P in soils at the east and west sites in the surface soil layers at a depth of 0-0.15 m (Table 1), where cluster roots grow, exude carboxylates and acquire P (Shane & Lambers, 2005). Therefore, adequate P in the surface soil layers is essential for the occurrence of *G. thelemanniana*, which needs more P than most other Australian Proteaceae.

Calcium requirement of *G. thelemanniana*

Most Proteaceae in south-western Australia inhabit old nutrient-impoverished soils with low available soil Ca, and are calcifuge, while only a few occur on young calcareous soils (Zemunik *et al.*, 2016; Hayes *et al.*, 2019a; Hayes *et al.*, 2019b). In the soil profile of east and west sites at Alison Baird Reserve, there was a considerably large amount of exchangeable Ca below 2 m from the soil surface (Table 1), where *G. thelemanniana* acquired water (Fig. 2). As Ca can move to the surface of roots together with water by mass flow due to 'solvent drag' created by transpiration (Barber & Ozanne, 1970), as well as diffusion of Ca from ground water to perched rain water in waterlogged soils in winter, *G. thelemanniana* had access to abundant Ca in this habitat. Our findings show that the leaf Ca concentration in *G. thelemanniana* was about 10 times greater than that in other Proteaceae (Fig. 3c), suggesting this species is calcicole, unlike most Proteaceae. To test the Ca requirement of *G. thelemanniana*, we conducted a hydroponic experiment using

different Ca treatments in which we included *B. telmatiaea*, which co-occurs with *G. thelemanniana* in the winter-wet low-lying areas in the field. In both species, Ca concentrations in leaves, stems and roots increased with increasing Ca supply (Fig. 5a), but the increase in leaf Ca concentration in *G. thelemanniana* was more pronounced than that in *B. telmatiaea*. Large amounts of Ca accumulated in the vacuoles of the epidermal cells, rather than being deposited as Ca oxalate crystals as in other plants. In contrast, *B. telmatiaea* stored most of the extra Ca in stems and roots. Plant dry weight, P_n and leaf N concentration in both species increased with greater leaf Ca concentrations (Fig. 5a), indicating a beneficial effect of Ca for the growth of *G. thelemanniana*.

Sodium intolerance of *G. thelemanniana*

There was abundant Na in the soil profiles of low-lying eastern and western sites of the reserve below 2 m from the surface (Table 1), and thus *G. thelemanniana* had no access to Na-free fresh ground water. However, leaf Na concentrations in the natural habitat were much lower in *G. thelemanniana* than in the other Proteaceae including *B. telmatiaea* (Fig. 3d). This suggests that *G. thelemanniana* excluded Na from its leaves, presumably due to (1) reduced Na uptake by roots due to greater selectivity (reduced influx), (2) exclusion of Na by roots due to greater efflux, and/or (3) reduced net transport of Na to leaves. In the hydroponics study, leaf [Na] increased in both species with increasing Na supply; however, plant biomass production was only reduced in *G. thelemanniana* (Fig. 4), indicating that *G. thelemanniana* was more salt sensitive than *B. telmatiaea*. High Na supply also increased leaf water content and reduced leaf osmotic potential in both species, with the effect being greater in *G. thelemanniana*. Obviously, *G. thelemanniana* is an extremely Na-sensitive species, similar to the most salt-sensitive crop species (Munns & Gilliham, 2015). As expected, this stress of high Na concentration negatively affected photosynthetic capacity, transpiration rate, F_v/F_m and Φ_{PSII} pf *G. thelemanniana* (Fig. 4).

The role of Ca in diminishing Na influx and accumulation

Supplemental Ca ameliorates Na stress in some plant species (Akhavan‐Kharazian *et al.*, 1991;

Cramer, 2002; Shabala *et al.*, 2006). To study the differences in response to Na stress between *G. thelemanniana* and *B. telmatiaea*, which co-occur in the field, and the effect of Ca supply on Na effects, we conducted a hydroponic experiment with different combinations of Na and Ca levels. In both *G. thelemanniana* and *B. telmatiaea,* addition of Ca significantly reduced Na uptake; however, it was more pronounced for *G. thelemanniana.* Reduction of Na influx by Ca treatment alleviated salt-induced inhibition of growth and accumulation in *G. thelemanniana*. Our findings clearly demonstrate that *G. thelemanniana* was extremely Na sensitive, and that supplemental Ca allowed it to exclude Na. This offers an explanation why *G. thelemanniana* is restricted to habitats with greater Ca availability.

The role of Ca in balancing accumulation of *trans*-aconitate

The most surprising and very exciting finding of this study was the accumulation of huge amounts of Ca in the leaves of *G. thelemanniana* which is unusual in Proteaceae (Hayes *et al.*, 2019b). Greater amounts of cellular free Ca may be toxic to plants and also precipitate PO_4^{3-}, reducing availability of both elements (Hayes *et al.*, 2019b). To avoid Ca toxicity, plants often biomineralise Ca by making crystals comprising calcium oxalate, calcium sulfate and calcium carbonate (He *et al.*, 2014; He *et al.*, 2015) . We detected abundant Ca crystals in all *Banksia* species that contained much lower Ca concentrations than *G. thelemanniana.* However, surprisingly, we hardly observed any Ca crystals in *G. thelemanniana*, which accumulated massive amounts of Ca in leaves compared with the *Banksia* species (Fig. 6). Instead of crystals, *G. thelemanniana* accumulated abundant non-mineralised Ca, mainly in its epidermal (EP) and spongy mesophyll (SM) cells (Fig. 7). Our subsequent investigation why *G. thelemanniana* accumulated enormous amounts of Ca without making crystals uncovered a novel and striking story on a calcicole species.

To accumulate Ca without producing crystals, it requires negative ions to balance the charge of Ca^{2+}. A comprehensive metabolite analysis revealed that *G. thelemanniana* leaves accumulated a large amount of aconitate (Fig. 7). As a carboxylate and negatively charged molecule, aconitate can chelate divalent cations such as Ca and Mg. Since *G. thelemanniana* leaves accumulated a

very large amount of *trans*-aconitate, which is a negative ion, it was essential to take up a large amount of Ca, a positive ion, to balance it inside leaf cells. Of the total amount of aconitate, 98% was *trans*-aconitate and its concentration in leaves of *G. thelemanniana* was more than 100 times greater than in the *Banksia* species (Fig. 7). We tested if this huge amount of *trans*-aconitate in was due to conversion of *cis*-aconitate during extraction. We falsified this, because, first, we carried out the extraction in ice, which minimised enzymatic reactions. Second, based on standards used through extraction and recovery/stability of *cis*- and *trans*- isomers we confirmed that conversion of the *cis*- to the *trans*- form was negligible. Since the *trans*-isomer is more stable than the *cis*-isomer, especially in acidic environment (Katsuhara *et al.*, 1993), an isomerase may promote accumulation of *trans*-aconitate in cells (Klinman & Rose, 1971; Igamberdiev & Eprintsev, 2016). It is likely that *trans*-aconitate is produced in the cytoplasm and then compartmentalised in vacuoles of epidermal cells, where we detected very high Ca concentrations.

Trans-aconitate is a stereoisomer of *cis*-aconitate, an intermediate of the tricarboxylic acid (TCA), and a potent inhibitor of aconitase in the TCA cycle (Saffran & Prado, 1949; Du *et al.*, 2017). It acts as a feeding deterrent (Burau & Stout, 1965; Kim *et al.*, 1976; Rustamani & Kanehisa, 1992; Katsuhara *et al.*, 1993) and in resistance to microbial pathogens (Pisano *et al.*, 1959). Remarkably, *G. thelemanniana* produced large amount of *trans*-aconitate, and thus required free Ca ions to balance the accumulation of *trans*-aconitate in leaves. This is the first report of this specific role of Ca in a calcicole species, but may well occur in other Proteaceae that exhibit high Ca concentrations in specific leaf cells, *e.g.*, *Lomatia* species (Hayes *et al.*, 2018).

In conclusion, our multi-facet research unraveled why the critically-endangered and threatened *G. thelemanniana* is a narrow endemic with a very restricted distribution. Our analyses revealed that *G. thelemanniana* (1) requires access to water year round including in the dry Mediterranean summer which restricts it to winter-wet low-lying flats. (2) It also operates at approximately 30% greater P levels than most Australian Proteaceae which limits its distribution to locations where soil P availability is slightly greater than in most habitats in south-western Australia. (3) Most importantly, unlike most Proteaceae, *G. thelemanniana* needs large amounts of Ca, but not

because this is sequestered in crystals, as in other Proteaceae, but to balance accumulation of a feeding-deterrent carboxylate, *trans*-aconitate in its leaves. As a result, *G. thelemanniana* is restricted to locations where soils have abundant Ca levels. This is the first discovery of a calcicole species requiring large amounts of Ca for this particular feature.

Acknowledgements

J.G. was supported by a scholarship from the China Scholarship Council (CSC) and F.W. was supported by a scholarship from the 100 Talents Program of Chongqing (20710940) to X.H. Funding was provided by research awards from UWA and a Future Fellowship (FT170100195) from the Australian Research Council (ARC) to K.R., and an Australian Research Council Discovery Grant (DP130100005) to H.L. and P.L.C. We thank Qi Shen for help with sample preparation, Robert Creasy and Bill Piasini for glasshouse support, and APACE nursery in Fremantle, WA for propagating *Grevillea thelemanniana* plants from stem cuttings. We acknowledge technical assistance from Lyn Kirilak and use of the Microscopy Australia facilities at the Centre for Microscopy, Characterisation & Analysis, The University of Western Australia, a facility funded by the University, State and Commonwealth Governments. The authors declare to have no competing interests.

Author contributions

K.R., H.L., and P.L.C. designed and supervised the study. J.G., F.W., A.J.A., M.L., H.Z., T.R. and G.R.C. worked on plant growth in the glasshouse, collected and prepared samples. J.G., F.W., A.J.A., M.L., H.Z., T.R., G.R.C., P.L.C., and K.R. performed the data analysis. J.G., F.W., K.R., H.L., and P.L.C. prepared the manuscript. K.R., H.L., X.H., M.L., H.Z., U.R., and G.R.C. revised the manuscript. All the authors read and approved the manuscript. J.G., F.W. and K.R. contributed equally to this work.

References

Akhavan‐Kharazian M, Campbell WF, Jurinak JJ, Dudley LM. 1991. Calcium amelioration of NaCl effects on plant rowth, chlorophyll, and ion concentration in *Phaseolus vulgaris*. *Arid Soil Research and Rehabilitation* **5**: 9-19.

Baker AJ, Ernst WH, van der Ent A, Malaisse F, Ginocchio R 2010. Metallophytes: the unique biological resource, its ecology and conservational status in Europe, central Africa and Latin America. In: Batty LC, Hallberg KB eds. *Ecology of Iindustrial Pollution*. Cambridge: Cambridge University Press, 7-39.

Barber SA, Ozanne PG. 1970. Autoradiographic evidence for the differential effect of four plant species in altering the calcium content of the rhizosphere soil. *Soil Science Society of America Journal* **34**: 635-637.

Bothe H. 2015. The lime–silicate question. *Soil Biology and Biochemistry* **89**: 172-183.

Brooks RR, ed. 1998. *Plants that Hyperaccumulate Heavy Metals. Their Role in Phytoremediation, Microbiology, Archaeology, Mineral Exploitation and Phytomining*. Wallingford: CAB International.

Burau R, Stout PR. 1965. Trans-aconitic acid in range grasses in early spring. *Science* **150**: 766-767.

Canham CA, Froend RH, Stock WD. 2009. Water stress vulnerability of four *Banksia* species in contrasting ecohydrological habitats on the Gnangara Mound, Western Australia. *Plant, Cell and Environment* **32**: 64-72.

Cawthray GR. 2003. An improved reversed-phase liquid chromatographic method for the analysis of low-molecular mass organic acids in plant root exudates. *Journal of Chromatography A* **1011**: 233-240.

Coplen TB. 1994. Reporting of stable hydrogen, carbon, and oxygen isotopic abundances (technical report). *Pure and Applied Chemistry* **66**: 273-276.

Cramer GR 2002. Sodium-calcium interactions under salinity stress. In: Läuchli A, Lüttge U eds. *Salinity: Environment-Plants-Molecules*. Dordrecht: Kluwer, 205-227.

Darwin CR. 1845. *Journal of Researches into the Natural History and Geology of the Countries Visited during the Voyage of H.M.S. Beagle Round the World, under the Command of Capt. Fitz Roy, R.N. 2d edition*. London: John Murray.

de Souza MC, Williams TCR, Poschenrieder C, Jansen S, Pinheiro MHO, Soares IP, Franco AC. 2020. Calcicole behaviour of *Callisthene fasciculata* Mart., an Al-accumulating species from the Brazilian Cerrado. *Plant Biology* **22**: 30-37.

Du C, Cao S, Shi X, Nie X, Zheng J, Deng Y, Ruan L, Peng D, Sun M. 2017. Genetic and biochemical characterization of a gene operon for *trans*-aconitic acid, a novel nematicide from *Bacillus thuringiensis*. *Journal of Biological Chemistry* **292**: 3517-3530.

Ehleringer JR, Dawson TE. 1992. Water uptake by plants: perspectives from stable isotope composition. *Plant, Cell and Environment* **15**: 1073-1082.

Escudero A, Palacio S, Maestre FT, Luzuriaga AL. 2015. Plant life on gypsum: a review of its multiple facets. *Biological Reviews* **90**: 1-18.

Gentilli J. 1972. *Australian Climate Patterns*. Melbourne: Thomas Nelson.

Genty B, Briantais J-M, Baker NR. 1989. The relationship between the quantum yield of photosynthetic electron transport and quenching of chlorophyll fluorescence. *Biochimica et Biophysica Acta - General Subjects* **990**: 87-92.

Good SP, Mallia DV, Lin JC, Bowen GJ. 2014. Stable isotope analysis of precipitation samples obtained via crowdsourcing reveals the spatiotemporal evolution of Superstorm Sandy. *PLoS ONE* **9**: e91117-e91117.

Hatton TJ, Ruprecht J, George RJ. 2003. Preclearing hydrology of the Western Australia wheatbelt: target for the future. *Plant and Soil* **257**: 341-356.

Hayes PE, Clode PL, Guilherme Pereira C, Lambers H. 2019a. Calcium modulates leaf cell-specific phosphorus allocation in Proteaceae from south-western Australia. *Journal of Experimental Botany* **70**: 3995–4009.

Hayes PE, Clode PL, Oliveira RS, Lambers H. 2018. Proteaceae from phosphorus-impoverished habitats preferentially allocate phosphorus to photosynthetic cells: an adaptation improving phosphorus-use efficiency. *Plant, Cell and Environment* **41**: 605–619.

Hayes PE, Guilherme Pereira C, Clode PL, Lambers H. 2019b. Calcium-enhanced phosphorus-toxicity in calcifuge and soil-indifferent Proteaceae along the Jurien Bay chronosequence. *New Phytologist* **221**: 764-777.

He H, Bleby TM, Veneklaas EJ, Lambers H, Kuo J. 2012. Morphologies and elemental compositions of calcium crystals in phyllodes and branchlets of *Acacia robeorum* (Leguminosae: Mimosoideae). *Annals of Botany* **109**: 887-896.

He H, Kirilak Y, Kuo J, Lambers H. 2015. Accumulation and precipitation of magnesium, calcium, and sulfur in two *Acacia* (Leguminosae; Mimosoideae) species grown in different substrates proposed for mine-site rehabilitation. *American Journal of Botany* **102**: 290-301.

He H, Veneklaas EJ, Kuo J, Lambers H. 2014. Physiological and ecological significance of biomineralization in plants. *Trends in Plant Science* **19**: 166-174.

Hevroy TH, Moody ML, Krauss SL, Gardner MG. 2013. Isolation, via 454 sequencing, characterization and transferability of microsatellites for *Grevillea thelemanniana* subsp. *thelemanniana* and cross-species amplification in the *Grevillea thelemanniana* complex (Proteaceae). *Conservation Genetics Resources* **5**: 887-890.

Hooker JD. 1847. On the vegetation of the Galapagos Archipelago, as compared with that of some other tropical islands and of the continent of America. *Transactions of the Linnean Society of London* **20**: 235-262.

Igamberdiev AU, Eprintsev AT. 2016. Organic acids: the pools of fixed carbon involved in redox regulation and energy balance in higher plants. *Frontiers in Plant Science* **7**: 1042.

Jefferies RL, Willis AJ. 1964. Studies on the calcicole-calcifuge habit: II. The Influence of calcium on the growth and establishment of four species in soil and sand cultures. *Journal of Ecology* **52**: 691-707.

Katsuhara M, Sakano K, Sato M, Kawakita H, Kawabe S. 1993. Distribution and production of trans-aconitic acid in barnyard grass (*Echinochloa crus-galli* var. *oryzicola*) as putative antifeedant against brown planthoppers. *Plant and Cell Physiology* **34**: 251-254.

Keerthisinghe G, Hocking PJ, Ryan PR, Delhaize E. 1998. Effect of phosphorus supply on the formation and function of proteoid roots of white lupin (*Lupinus albus* L.). *Plant, Cell and Environment* **21**: 467-478.

Kim M, Koh H-S, Obata T, Fukami H, Ishii S. 1976. Isolation and identification of *trans*-aconitic acid as the antifeedant in barnyard grass against the brown planthopper, (STAL) (Hompotara : Delphacidae). *Applied Entomology and Zoology* **11**: 53-57.

Klinman JP, Rose IA. 1971. Mechanism of the aconitate isomerase reaction. *Biochemistry* **10**: 2259-2266.

Kohn D, Murrell G, Parker J, Whitehorn M. 2005. What Henslow taught Darwin. *Nature* **436**: 643-645.

Kotula L, Clode PL, Jimenez JDLC, Colmer TD. 2019. Salinity tolerance in chickpea is associated with the ability to 'exclude' Na from leaf mesophyll cells. *Journal of Experimental Botany* **70**: 4991-5002.

Kruckeberg AR, Rabinowitz D. 1985. Biological aspects of endemism in higher plants. *Annual Review of Ecology and Systematics* **16**: 447-479.

Lambers H, ed. 2014. *Plant Life on the Sandplains in Southwest Australia, a Global Biodiversity Hotspot*. Crawley, Australia: University of Western Australia Publishing.

Lambers H, Albornoz F, Kotula L, Laliberté E, Ranathunge K, Teste FP, Zemunik G. 2018. How belowground interactions contribute to the coexistence of mycorrhizal and non-mycorrhizal species in severely phosphorus-impoverished hyperdiverse ecosystems. *Plant and Soil* **424**: 11-34.

Lambers H, Cawthray GR, Giavalisco P, Kuo J, Laliberté E, Pearse SJ, Scheible W-R, Stitt M, Teste F, Turner BL. 2012. Proteaceae from severely phosphorus-impoverished soils extensively replace phospholipids with galactolipids and sulfolipids during leaf development to achieve a high photosynthetic phosphorus-use efficiency. *New Phytologist* **196**: 1098-1108.

Lambers H, Finnegan PM, Jost R, Plaxton WC, Shane MW, Stitt M. 2015. Phosphorus nutrition in Proteaceae and beyond. *Nature Plants* **1**: 15109.

Lane P, Evans KA 2019. Geology of the proposed Yule Brook Regional Park. In: Lambers H ed. *A Jewel in the Crown of a Global Biodiversity Hotspot*. Perth: Kwongan Foundation and the Western Australian Naturalists' Club Inc, 23-31.

Lee JA. 1998. The calcicole—calcifuge problem revisited. *Advances in Botanical Research* **29**: 1-30.

McLaughlin SB, Wimmer R. 1999. Calcium physiology and terrestrial ecosystem processes. *New Phytologist* **142**: 373-417.

Motomizu S, Wakimoto T, Toei K. 1983. Spectrophotometric determination of phosphate in river waters with molybdate and malachite green. *Analyst* **108**: 361-367.

Munns R, Gilliham M. 2015. Salinity tolerance of crops – what is the cost? *New Phytologist* **208**: 668-673.

Myers N, Mittermeier RA, Mittermeier CG, da Fonseca GAB, Kent J. 2000. Biodiversity hotspots for conservation priorities. *Nature* **403**: 853-858.

Pavlik BM. 1980. Patterns of water potential and photosynthesis of desert sand dune plants, Eureka Valley, California. *Oecologia* **46**: 147-154.

Peltzer D, Wardle D, Allison V, Baisden W, Bardgett R, Chadwick O, Condron L, Parfitt R, Porder S, Richardson S, Turner B, Vitousek P, Walker J, Walker L. 2010. Understanding ecosystem retrogression. *Ecological Monographs* **80**: 509-529.

Pisano MA, Blahuta GJ, Mullen GA. 1959. Selective antibacterial activity of aconitic acid. *Journal of Bacteriology* **78**: 146-146.

Poot P, Bakker R, Lambers H. 2008. Adaptations to winter-wet ironstone soils: a comparison between rare ironstone *Hakea* (Proteaceae) species and their common congeners. *Australian Journal of Botany* **56**: 574-582.

Poot P, Lambers H. 2008. Shallow-soil endemics: adaptive advantages and constraints of a specialized root-system morphology. *New Phytologist* **178**: 371-381.

Rayment GE, Higginson FR. 1992. *Australian Laboratory Handbook of Soil and Water Chemical Methods*. Melbourne, Australia: Inkata Press.

Rayment GE, Lyons DJ. 2011. *Soil chemical methods - Australasia*. Collingwood, Australia: CSIRO Publishing.

Rustamani MA, Kanehisa K. 1992. Further observations on the relationship between aconitic acid contents and aphid densities. *Bull. Res. Inst. Bioresour. Okayama Univ* **1**: 9-20.

Ryżak M, Bieganowski A. 2011. Methodological aspects of determining soil particle-size distribution using the laser diffraction method. *Journal of Plant Nutrition and Soil Science* **174**: 624-633.

Saffran M, Prado JL. 1949. Inhibition of aconitase by *trans*-aconitate. *Journal of Biological Chemistry* **180**: 1301-1309.

Salmerón-Sánchez E, Martínez-Nieto MI, Martínez-Hernández F, Garrido-Becerra JA, Mendoza-Fernández AJ, de Carrasco CG, Ramos-Miras JJ, Lozano R, Merlo ME, Mota JF. 2014. Ecology, genetic diversity and phylogeography of the Iberian endemic plant *Jurinea pinnata* (Lag.)

DC. (Compositae) on two special edaphic substrates: dolomite and gypsum. *Plant and Soil* **374**: 233-250.

Schad P, van Huyssteen C, Micheli E, eds. 2014. *IUSS Working Group, World Reference Base for Soil Resources, World Soil Resources Reports No. 106, 189 p.* Rome: FAO.

Shabala S, Demidchik V, Shabala L, Cuin TA, Smith SJ, Miller AJ, Davies JM, Newman IA. 2006. Extracellular Ca^{2+} ameliorates NaCl-induced K^+ loss from *Arabidopsis* root and leaf cells by controlling plasma membrane K^+-permeable channels. *Plant Physiology* **141**: 1653-1665.

Shane MW, Lambers H. 2005. Cluster roots: a curiosity in context. *Plant and Soil* **274**: 101-125.

Sperry JS, Donnelly JR, Tyree MT. 1988. A method for measuring hydraulic conductivity and embolism in xylem. *Plant, Cell and Environment* **11**: 35-40.

Tansley AG. 1917. On competition between *Galium saxatile* L. (*G. hercynicum* Weig.) and *Galium sylvestre* Poll. (*G. asperum* Schreb.) on different types of soil. *Journal of Ecology* **5**: 173-179.

Tauss C, Keighery GJ, Keighery BJ, Cloran PM, Genovese SD 2019. A new look at the flora and the vegetation patterns of the Greater Brixton Street Wetlands and Yule Brook. In: Lambers H ed. *A Jewel in the Crown of a Global Biodiversity Hotspot*. Perth: Kwongan Foundation and the Western Australian Naturalists' Club Inc, 69-207.

Turner BL, Laliberté E. 2015. Soil development and nutrient availability along a 2 million-year coastal dune chronosequence under species-rich Mediterranean shrubland in southwestern Australia. *Ecosystems* **18**: 287-309.

Tyree MT, Sperry JS. 1989. Vulnerability of xylem to cavitation and embolism. *Annual Review of Plant Physiology and Molecular Biology* **40**: 19-36.

Walker TW, Syers JK. 1976. The fate of phosphorus during pedogenesis. *Geoderma* **15**: 1-9.

Whittaker RH. 1954. The ecology of serpentine soils. I. Introduction. *Ecology* **35**: 258-259.

Wright IJ, Reich PB, Westoby M, Ackerly DD, Baruch Z, Bongers F, Cavender-Bares J, Chapin T, Cornelissen JHC, Diemer M, Flexas J, Garnier E, Groom PK, Gulias J, Hikosaka K, Lamont BB, Lee T, Lee W, Lusk C, Midgley JJ, Navas M-L, Niinemets Ü, Oleksyn J, Osada N, Poorter H, Poot P, Prior L, Pyankov VI, Roumet C, Thomas SC, Tjoelker MG, Veneklaas EJ, Villar R. 2004. The worldwide leaf economics spectrum. *Nature* **428**: 821-827.

Zemunik G, Turner BL, Lambers H, Laliberté E. 2016. Increasing plant species diversity and extreme species turnover accompany declining soil fertility along a long-term chronosequence in a biodiversity hotspot. *Journal of Ecology* **104**: 792-805.

Zhang Y, Lamarque LJ, Torres-Ruiz JM, Schuldt B, Karimi Z, Li S, Qin D-W, Bittencourt P, Burlett R, Cao K-F, Delzon S, Oliveira R, Pereira L, Jansen S. 2018. Testing the plant pneumatic method to estimate xylem embolism resistance in stems of temperate trees. *Tree Physiology* **38**: 1016–1025.

Supporting information:

Fig. S1: Growth of *Grevillea thelemanniana* and *Banksia telmatiaea* under different calcium concentrations.

Fig. S2: Growth of *Grevillea thelemanniana* and *Banksia telmatiaea* under different calcium and sodium concentrations.

Fig. S3: Qualitative element maps of oxygen and silicon crystals (phytoliths) in epidermal cells of *Banksia telmatiaea* and *Banksia attenuata*.

Table S1: List of salient features of *Grevillea thelemanniana*, *Banksia telmatiaea*, *Banksia attenuata* and *Banksia menziesii*.

Fig. 1. (a) Location of Alison Baird Reserve in Yule Brook where four studied Proteaceae species occur naturally; the reserve is located about 20 km from Perth. The inset shows the global biodiversity hotspot of south-western Australia. (b) The collection sites of the four Proteaceae. Eastern and western winter-wet low-lying sites (yellow and purple) where *Grevillea thelemanniana* and *Banksia telmatiaea* occur. Top of a 2-million year old, 5 m high Bassendean sand dune (orange) where *Banksia menziesii* and *Banksia attenuata* occur. (c) Catena and habitats

of *Grevillea thelemanniana*, *Banksia telmatiaea*, *Banksia attenuata* and *Banksia menziesii*.

Fig. 2. Water relations of *Grevillea thelemanniana* (G.T.), *Banksia telmatiaea* (B.T.), *Banksia menziesii* (B.M.) and *Banksia attenuata* (B.A.) growing in Alison Baird Reserve in south-western Australia (Fig. 1). (a-d) Isotope composition of soil water and stem xylem sap of plants in winter and summer. The δ^2H_{liq} (a) and $\delta^{18}O_{liq}$ (b) in soil water collected from different depths between 0 and 5 m. The values of δ^2H_{liq} (c) and $\delta^{18}O_{liq}$ (d) in the stem xylem sap of four Proteaceae species. The water potential (e) and percent loss of hydraulic conductivity (PLC) of stems (f) of these species in summer and winter. Data are means ± SE (n = 4). Different letters indicate significant differences at $P < 0.05$, which was determined by Dunnett's multiple comparison test. G.T. East, G.T. West, B.T. East and B.T. West refer to *G. thelemanniana* and *B. telmatiaea* collected from the east and west of a sand dune, respectively.

Fig. 3. (a-d) Leaf nitrogen (N), phosphorus (P), calcium (Ca) and sodium (Na) concentrations of *Grevillea thelemanniana* (G.T.), *Banksia telmatiaea* (B.T.), *B. menziesii* (B.M.) and *B. attenuata* (B.A.) collected in Alison Baird Reserve in south-western Australia (Fig. 1). Concentrations are on a dry weight basis. Data are means ± SE (n = 4). Different letters indicate significant differences at $P < 0.05$, which was determined by Dunnett's multiple comparison test. G.T. East, G.T. West, B.T. East and B.T. West refer to *G. thelemanniana* and *B. telmatiaea* collected to the east and west of a sand dune, respectively.

Fig. 4. Combination of sodium (Na) and calcium (Ca) treatments on different plant physiological parameters; (a) plant dry weight, (b) leaf Na concentration, (c) leaf water content, (d) leaf osmotic potential, (e) net photosynthetic rate, (f) transpiration rate, (g) maximum quantum efficiency of photosystem II (F_v/F_m) and (h) quantum efficiency of PSII (Φ_{PSII}) of *Grevillea thelemanniana* and *Banksia telmatiaea* plants grown in aerated hydroponics for 30 days. Data are means ± SE (n = 4). Different letters indicate significant differences at $P < 0.05$, which was determined by Dunnett's

multiple comparison test.

Fig. 5. (a) Calcium concentrations ([Ca]) in leaves, stems and roots of *Grevillea thelemanniana* (G.T.) and *Banksia telmatiaea* (B.T.) grown in aerated hydroponics for eight weeks with different [Ca]. Data are means ± SE (n = 4). Different letters indicate significant differences at $P < 0.05$, which was determined by Dunnett's multiple comparison test. (b) Correlations between plant dry weights, net photosynthetic rate (P_n), leaf nitrogen (N) and phosphorus (P) concentrations and leaf [Ca] of *Grevillea thelemanniana* and *B. telmatiaea*. Each line represents the best fit for each species with grey regions indicating the 95% confidence interval, derived from a linear model.

Fig. 6. Maximum intensity projection X-ray microscopy images highlighting the presence of biominerals (appearing as bright, high-density features) within leaf tissues of *Grevillea thelemanniana*, *Banksia telmatiaea*, *B. menziesii*, and *B. attenuata*. Boxes highlight inset areas for each leaf. White arrowheads show abundant calcium-based crystals (presumed to be oxalates) in mesophyll cells of *Banksia* but only very occasionally in the epidermal cells of *Grevillea*. Black arrows show numerous silica-based crystals (presumed to be phytoliths) in the epidermal cells of *B. telmatiaea* and *B. attenuata*. Scale bars = 100 μm (*B. menziesii* and *B. attenuata*) and 200 μm (*G. thelemanniana* and *B. telmatiaea*).

Fig. 7. (a) Carboxylate concentrations in leaves of *Grevillea thelemanniana* and *Banksia telmatiaea* collected from Alison Baird Reserve in south-western Australia (Fig. 1). (b) Percentage of *cis*- and *trans*-aconitate of the total amount of aconitate in leaves of *G. thelemanniana* and *B. telmatiaea*. (c) Mean leaf cell-specific calcium (Ca) concentrations, which were quantified in different cell types; EP: epidermis, PM: palisade mesophyll, SM: spongy mesophyll. (d) Element maps showing oxygen distribution (O; for leaf anatomy) and cellular Ca concentrations of *G. thelemanniana* (G.T.) and *B. telmatiaea* (B.T.) leaves; scale bars = 50 μm. Calcium concentration is shown on a linear scale (black = not detectable to white = >500 mmol kg^{-1}). All leaves were

isobilateral. Data are means ± SE (n = 4 plants, of which many cells were analysed). *$P < 0.05$, ** $P < 0.01$ and *** $P < 0.001$ levels. Different letters indicate significant differences at $P < 0.05$, which was determined by Dunnett's multiple comparison test.

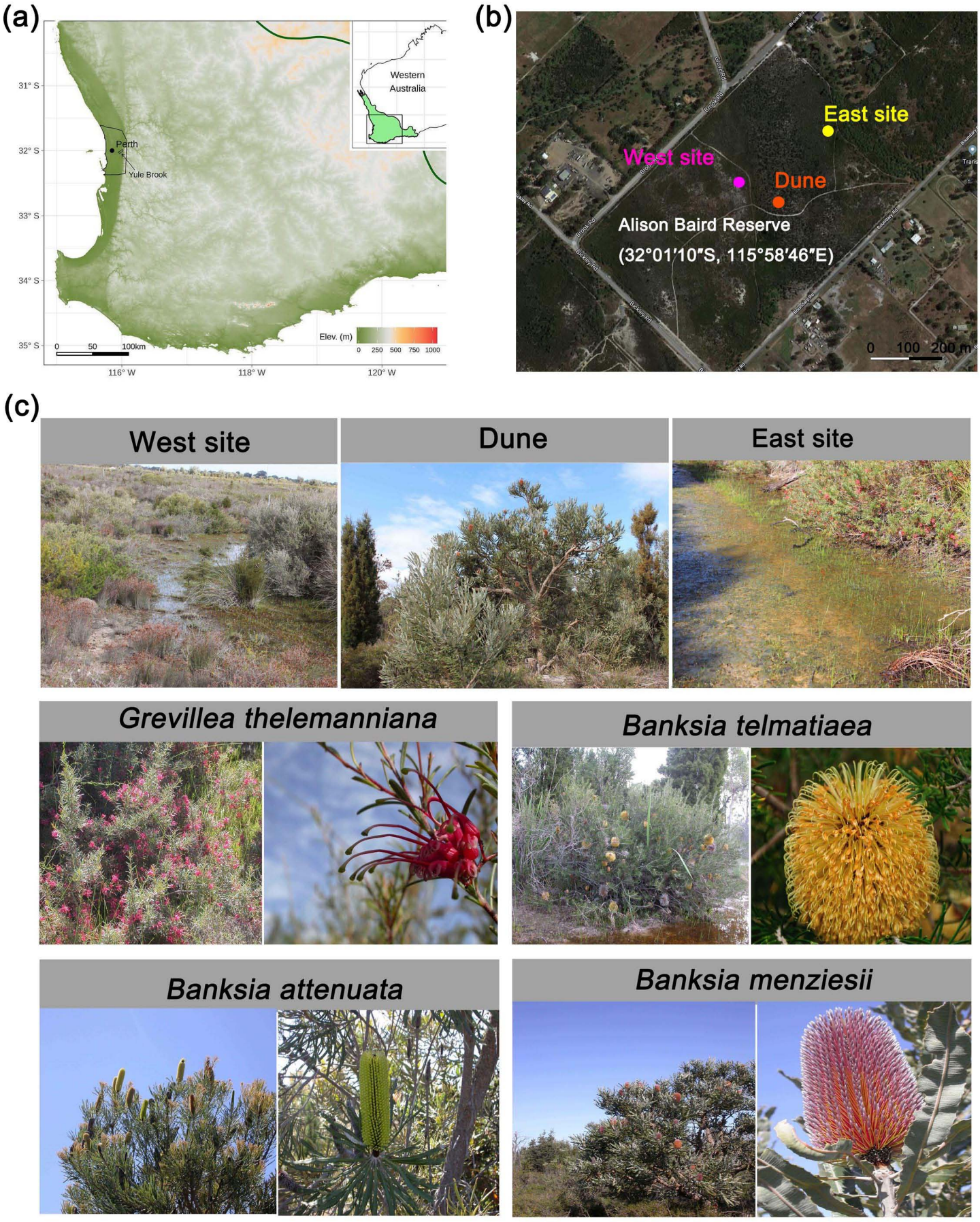
(a)
Western Australia
Perth
Yule Brook
31° S
32° S
33° S
34° S
35° S
0 50 100km
Elev. (m)
0 250 500 750 1000
116° W
118° W
120° W
(b)
East site
West site
Dune
Alison Baird Reserve
(32°01′10″S, 115°58′46″E)
0 100 200 m
(c)
West site
Dune
East site
Grevillea thelemanniana
Banksia telmatiaea
Banksia attenuata
Banksia menziesii

(a)

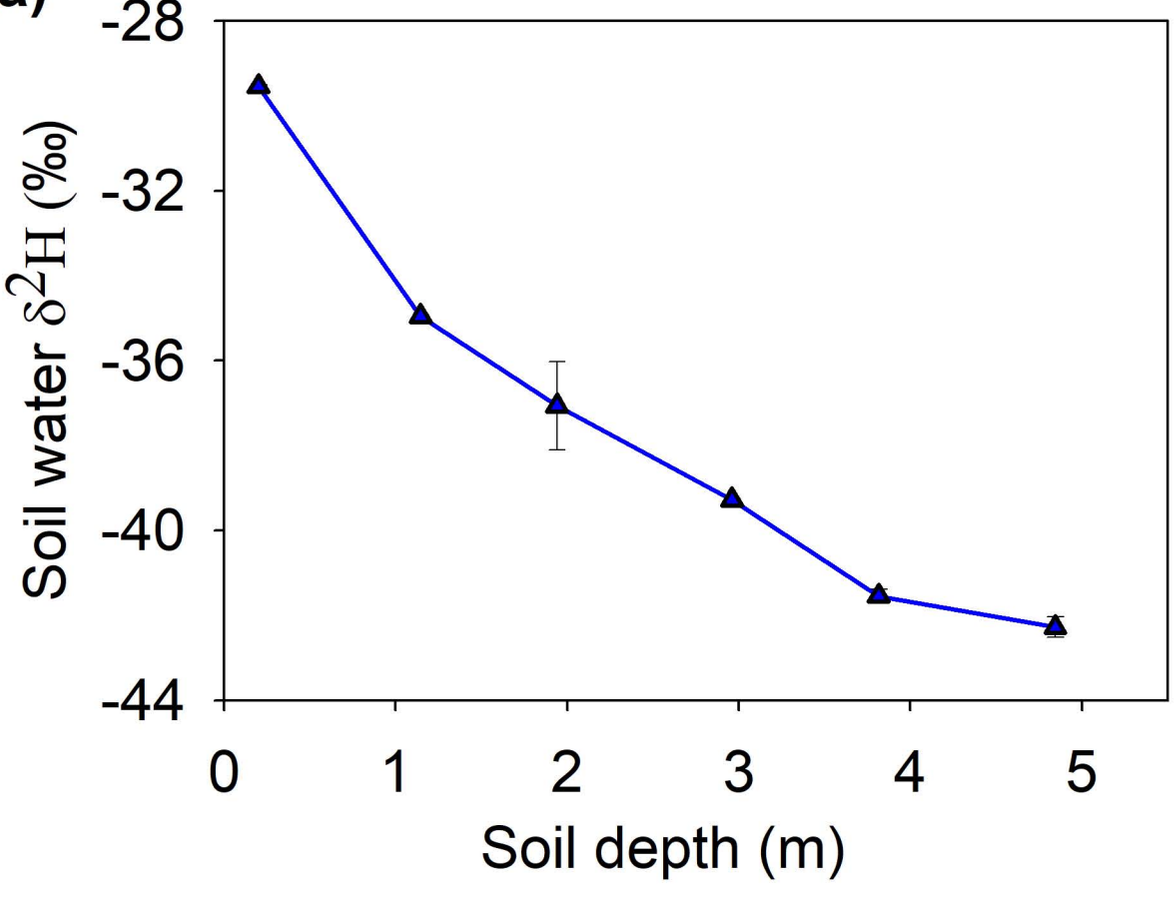
Soil water δ^2H (‰)
-28
-32
-36
-40
-44
0
1
2
3
4
5
Soil depth (m)

(b)

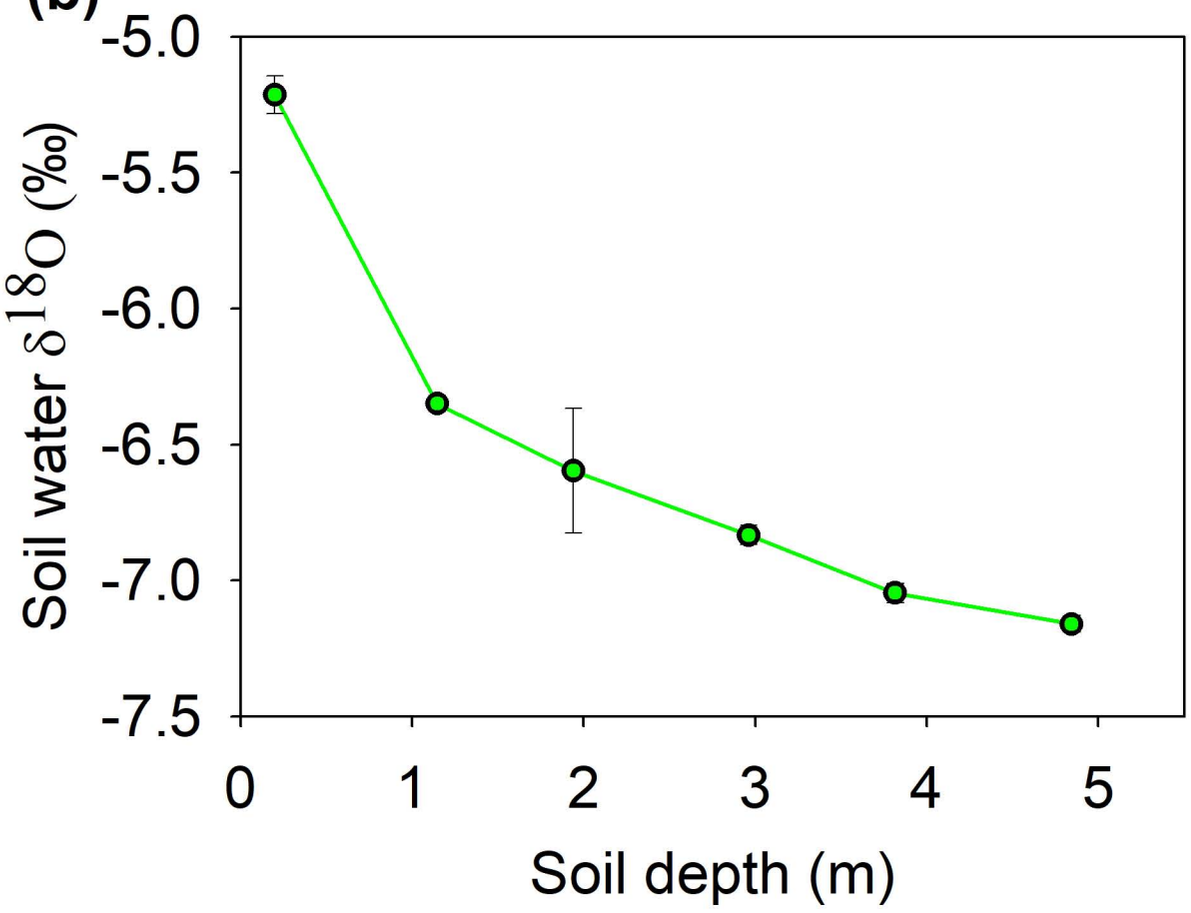
Soil water $\delta^{18}O$ (‰)
-5.0
-5.5
-6.0
-6.5
-7.0
-7.5
0
1
2
3
4
5
Soil depth (m)

(c)

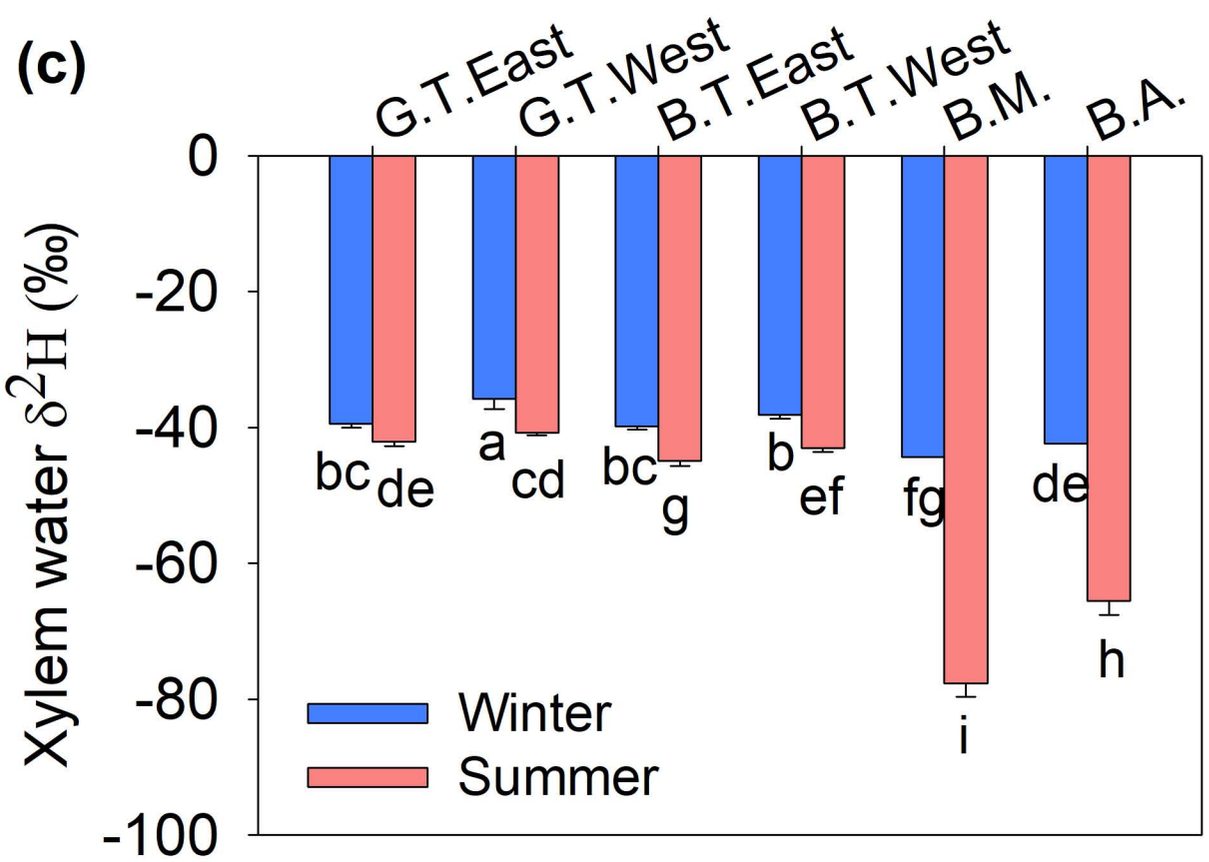
Xylem water δ^2H (‰)
0
-20
-40
-60
-80
-100
G.T.East
G.T.West
B.T.East
B.T.West
B.M.
B.A.
bc
de
a
cd
bc
g
b
ef
fg
i
de
h
Winter
Summer

(d)

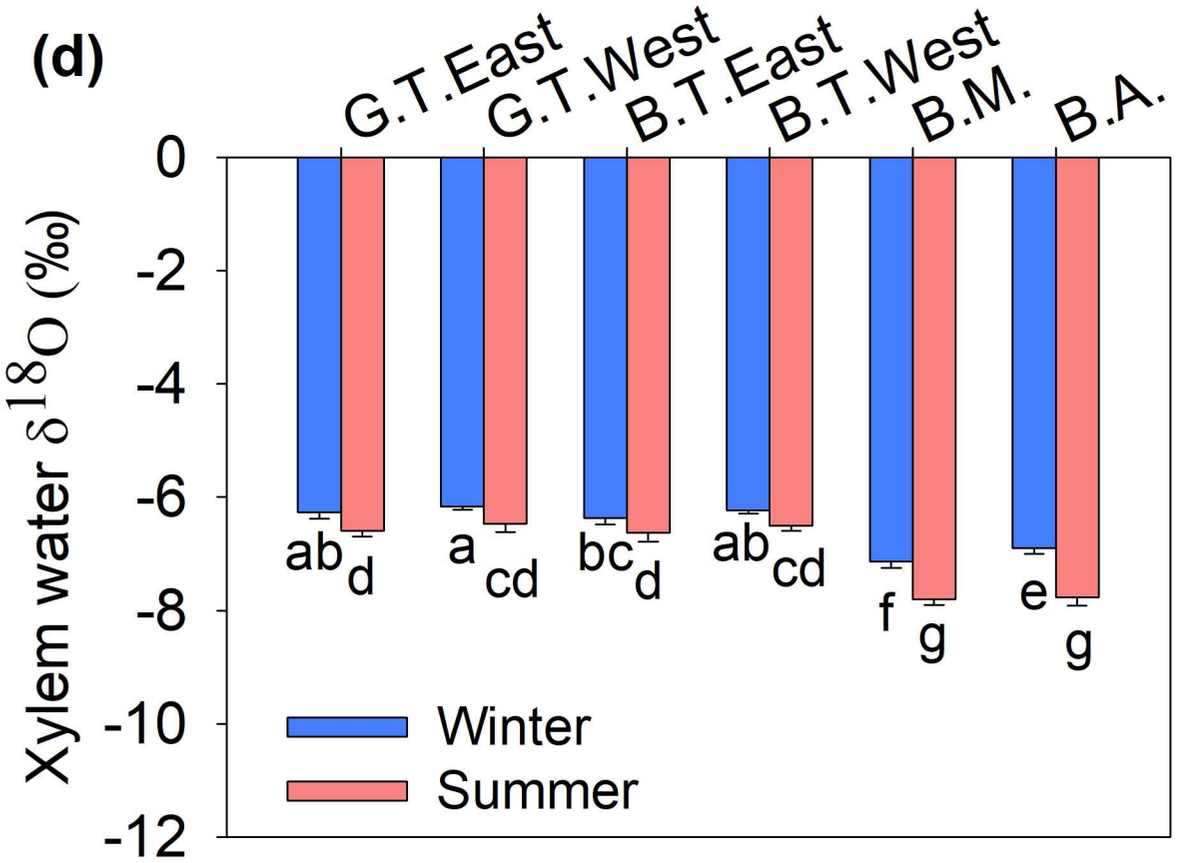
Xylem water $\delta^{18}O$ (‰)
0
-2
-4
-6
-8
-10
-12
G.T.East
G.T.West
B.T.East
B.T.West
B.M.
B.A.
ab
d
a
cd
bc
d
ab
cd
f
g
e
g
Winter
Summer

(e)

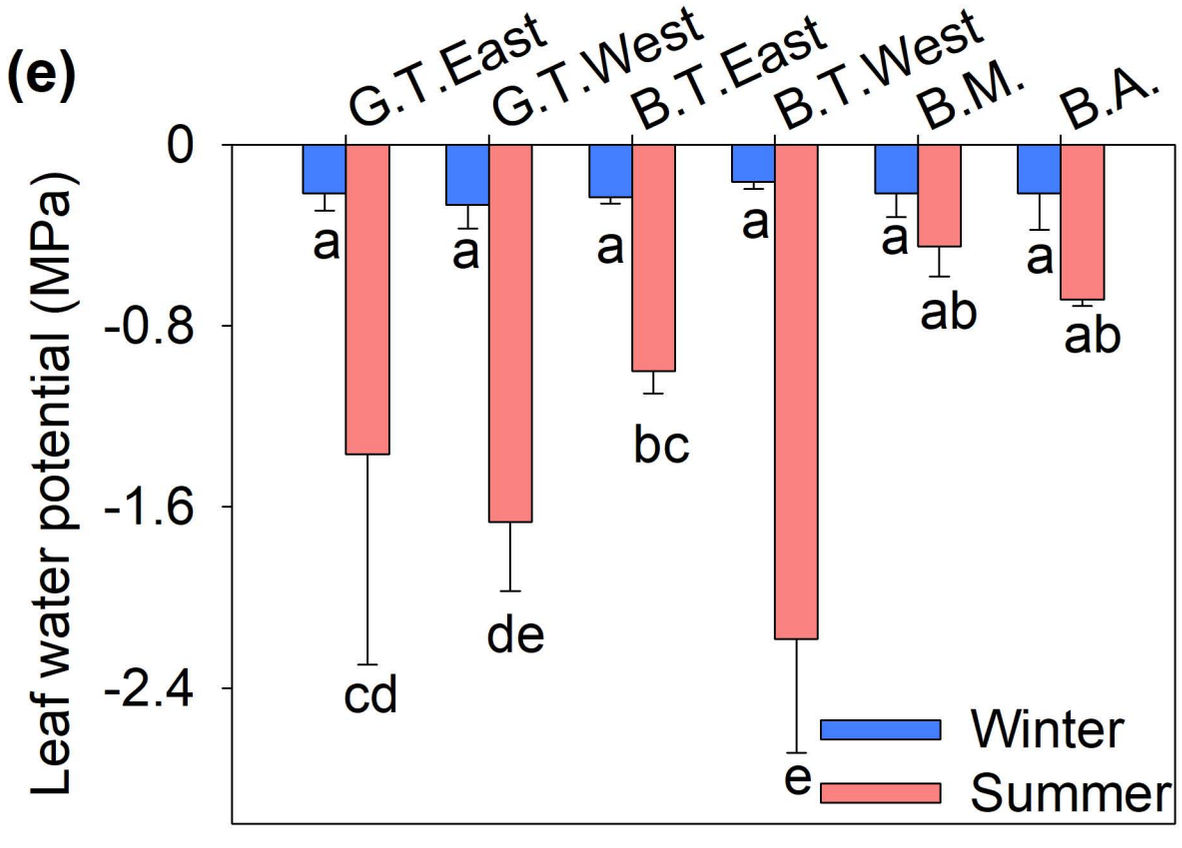
Leaf water potential (MPa)
0
-0.8
-1.6
-2.4
G.T.East
G.T.West
B.T.East
B.T.West
B.M.
B.A.
a
cd
a
de
a
bc
a
e
a
ab
a
ab
Winter
Summer

(f)

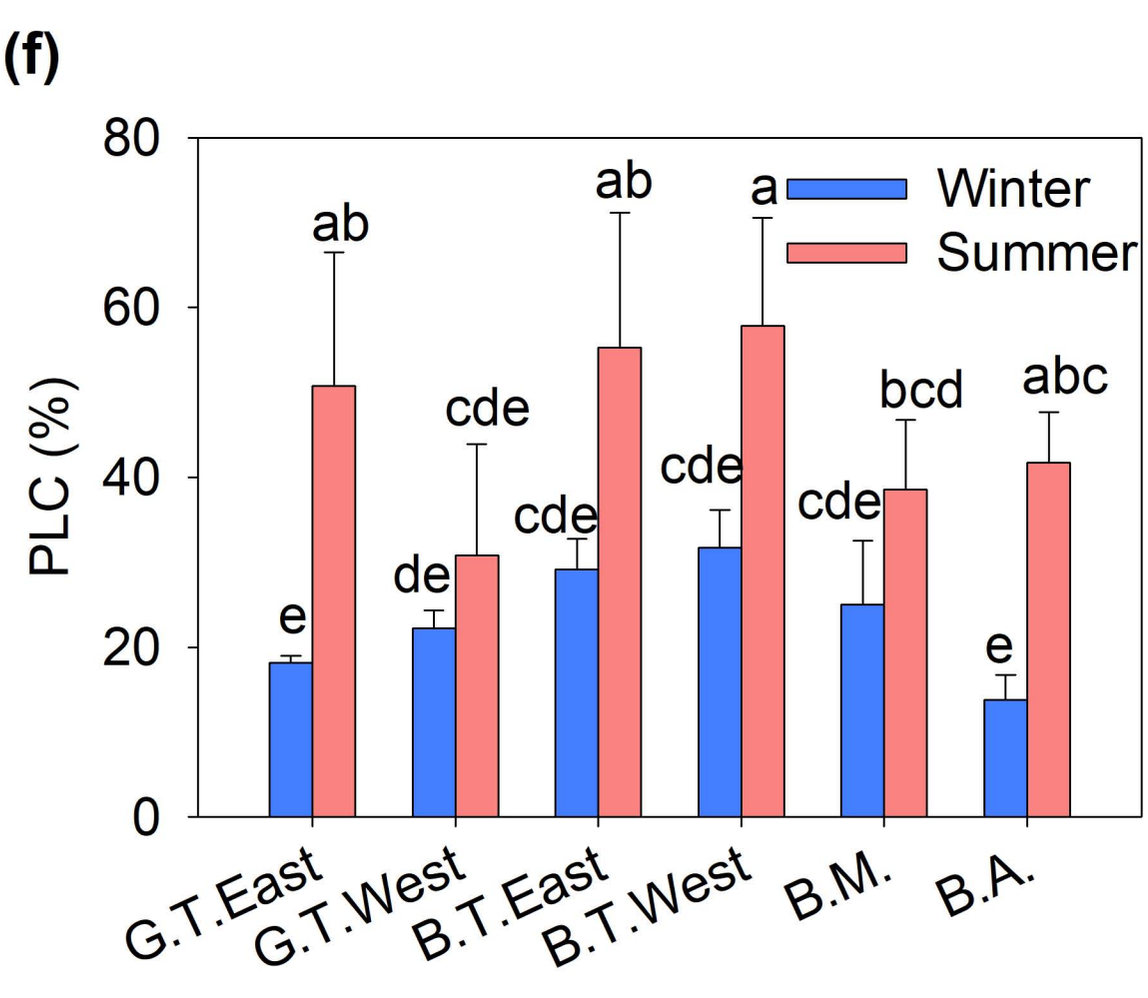
PLC (%)
80
60
40
20
0
ab
e
cde
de
cde
ab
cde
a
cde
bcd
e
abc
Winter
Summer
G.T.East
G.T.West
B.T.East
B.T.West
B.M.
B.A.

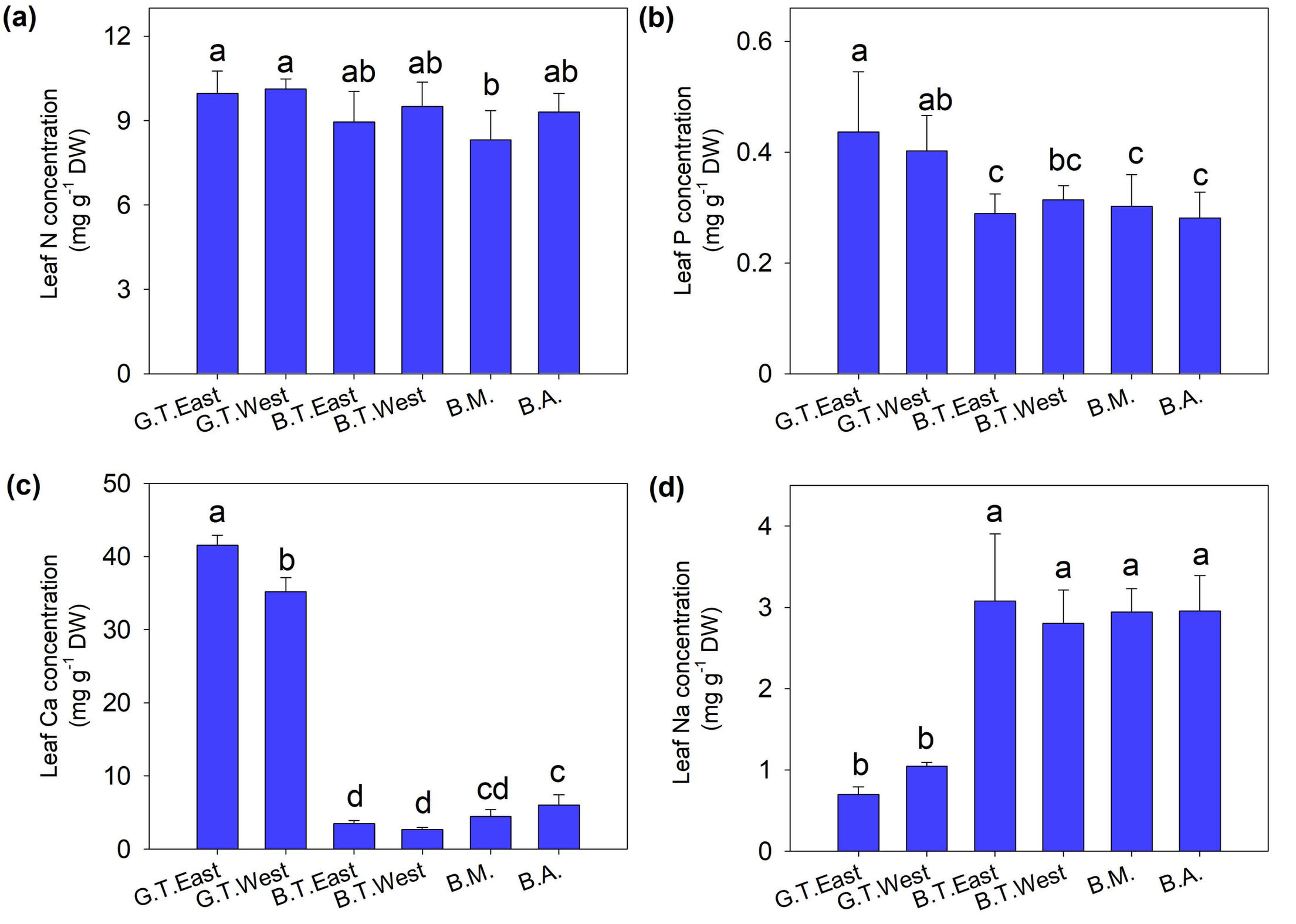
(a)
Leaf N concentration (mg g-1 DW)
12
9
6
3
0
a
a
ab
ab
b
ab
G.T.East
G.T.West
B.T.East
B.T.West
B.M.
B.A.
(b)
Leaf P concentration (mg g-1 DW)
0.6
0.4
0.2
0
a
ab
c
bc
c
c
G.T.East
G.T.West
B.T.East
B.T.West
B.M.
B.A.
(c)
Leaf Ca concentration (mg g-1 DW)
50
40
30
20
10
0
a
b
d
d
cd
c
G.T.East
G.T.West
B.T.East
B.T.West
B.M.
B.A.
(d)
Leaf Na concentration (mg g-1 DW)
4
3
2
1
0
b
b
a
a
a
a
G.T.East
G.T.West
B.T.East
B.T.West
B.M.
B.A.

(a)

Grevillea thelemanniana

Banksia telmatiaea

0.1 mM Ca

1.2 mM Ca

Plant dry weight (g plant^{-1})

6

4

2

0

ab a cd bc d bc a a a a a a

(b)

Grevillea thelemanniana

Banksia telmatiaea

0.1 mM Ca

1.2 mM Ca

Leaf Na concentration (mg g^{-1} DW)

0.9

0.6

0.3

0

e e b d a c c c b b a b

(c)

Leaf water content (%)

90

60

30

0

b ab ab ab a ab a a a a a a

(d)

Leaf osmotic potential (MPa)

0

-0.4

-0.8

-1.2

a a c a d b a a bc a c ab

(e)

Net photosynthetic rate (μmol CO_2 m^{-2} s^{-1})

45

30

15

0

a a bc ab c ab bc ab bc a c ab

(f)

Transpiration rate (mmol H_2O m^{-2} s^{-1})

20

15

10

5

0

a a bc b c b ab a a a b a

(g)

Fv/Fm

1.2

0.8

0.4

0

bc a c b d bc a a a a a a

(h)

Φ_{PSII}

0.9

0.6

0.3

0

ab a bc ab c ab a a a a a a

0 5 10 0 5 10

Na treatment (mM)

0 5 10 0 5 10

Na treatment (mM)

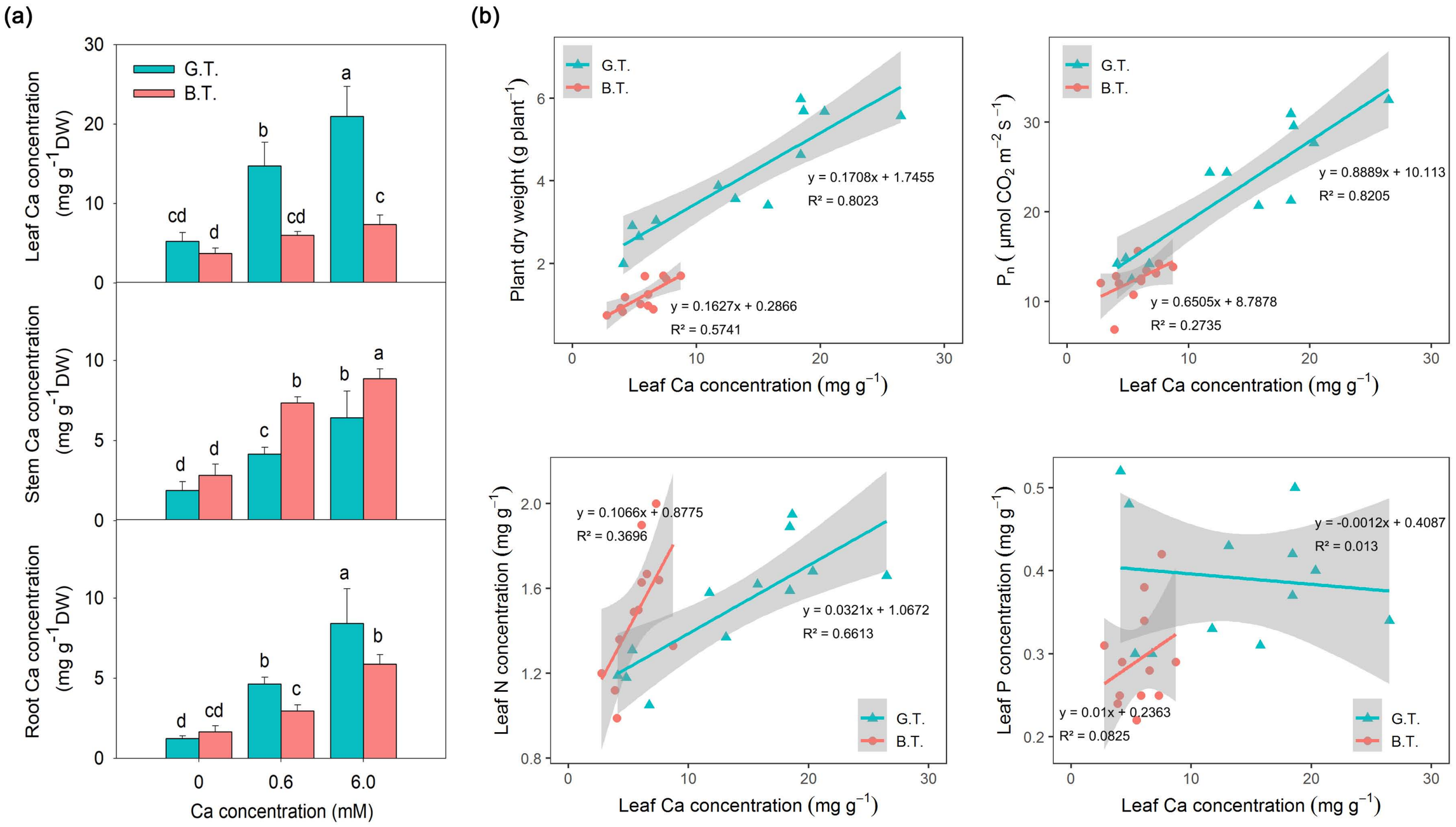
(a)
G.T.
B.T.
Leaf Ca concentration (mg g-1DW)
Stem Ca concentration (mg g-1DW)
Root Ca concentration (mg g-1DW)
cd
d
b
cd
a
c
d
d
c
b
b
a
d
cd
b
c
a
b
0
0.6
6.0
Ca concentration (mM)
(b)
Plant dry weight (g plant-1)
y = 0.1708x + 1.7455
R² = 0.8023
y = 0.1627x + 0.2866
R² = 0.5741
Leaf Ca concentration (mg g-1)
Pn (μmol CO2 m-2 s-1)
y = 0.8889x + 10.113
R² = 0.8205
y = 0.6505x + 8.7878
R² = 0.2735
Leaf N concentration (mg g-1)
y = 0.1066x + 0.8775
R² = 0.3696
y = 0.0321x + 1.0672
R² = 0.6613
Leaf P concentration (mg g-1)
y = -0.0012x + 0.4087
R² = 0.013
y = 0.01x + 0.2363
R² = 0.0825

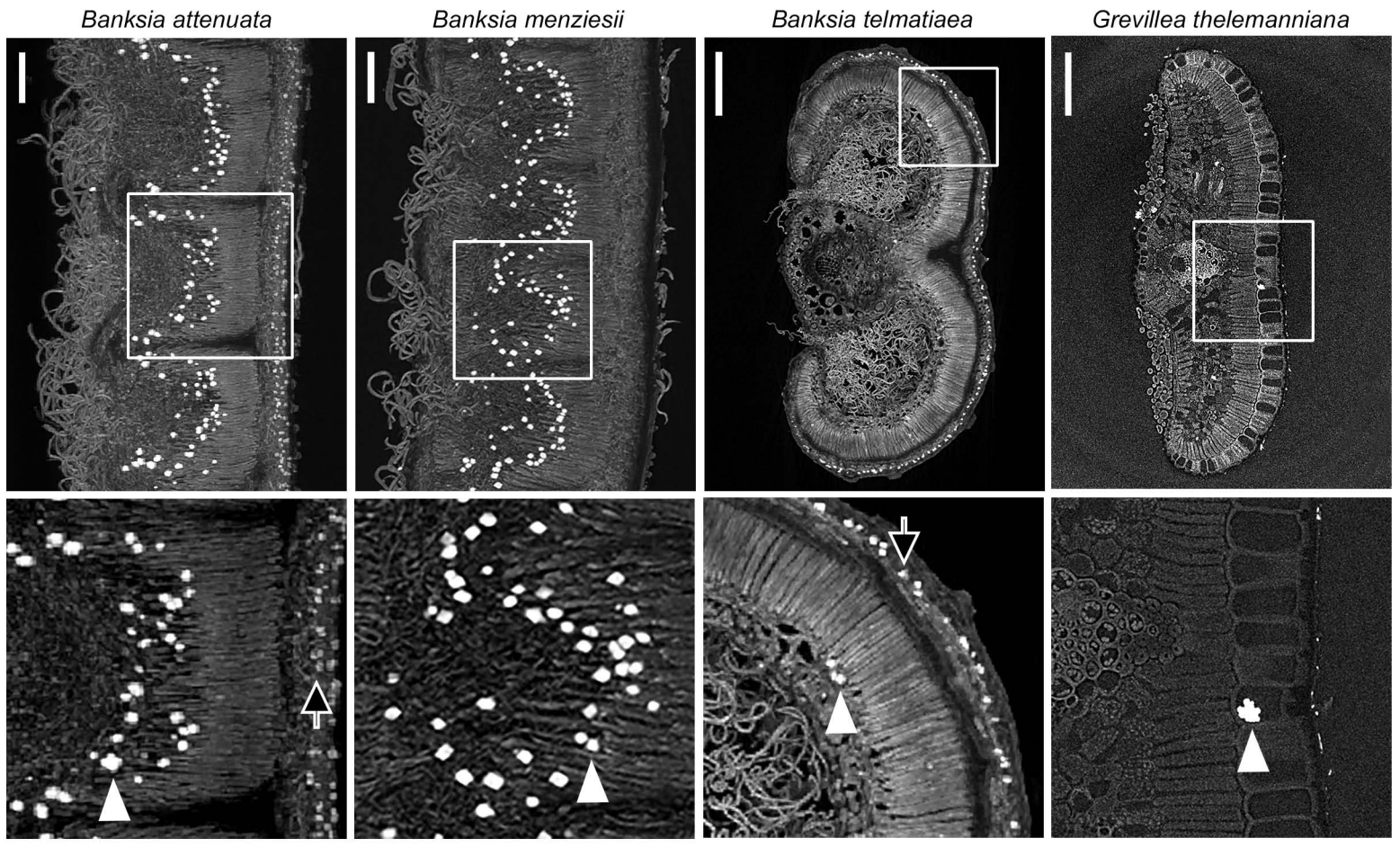
Banksia attenuata
Banksia menziesii
Banksia telmatiaea
Grevillea thelemanniana

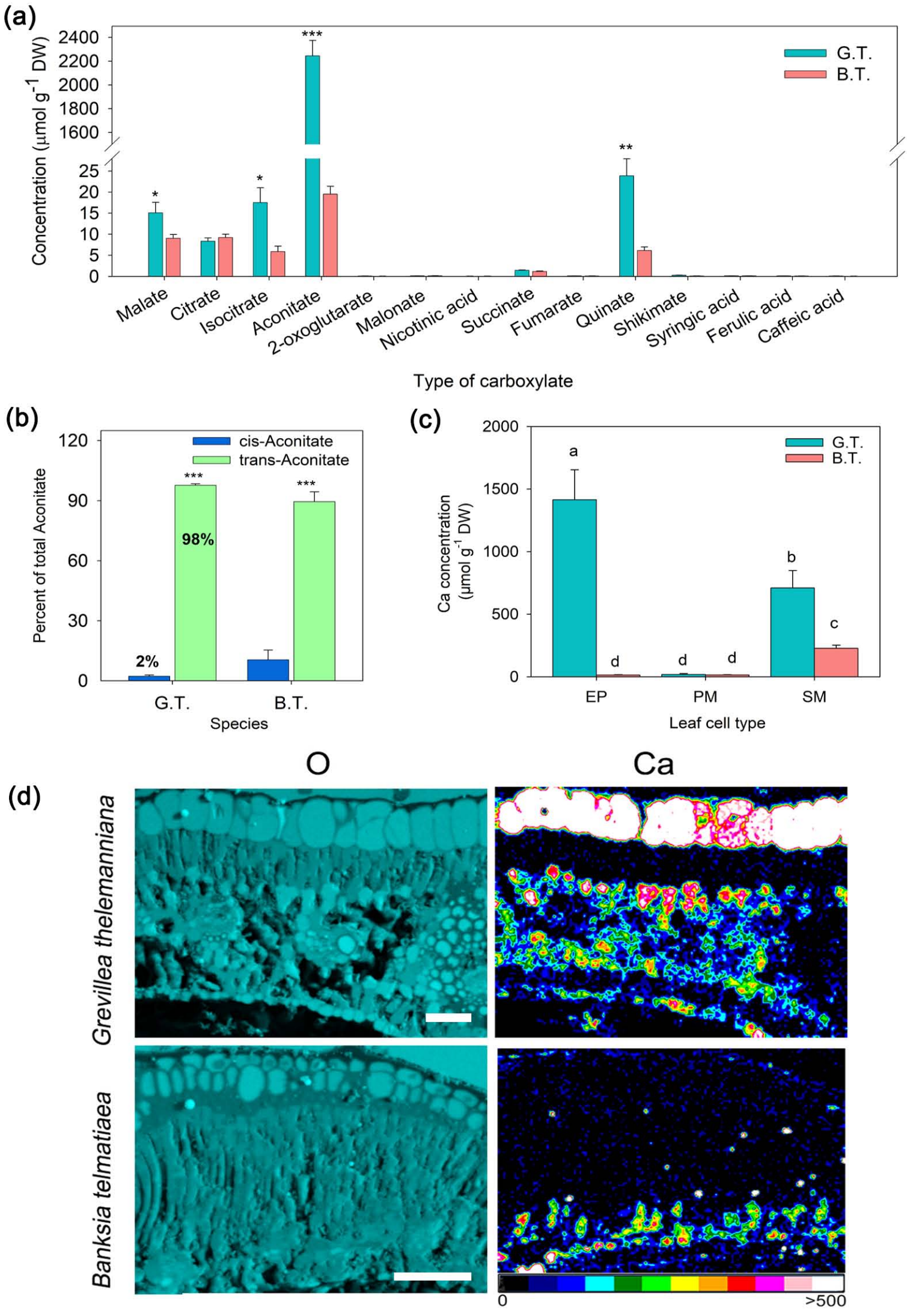
(a)
Concentration (μmol g-1 DW)
2400
2200
2000
1800
1600
25
20
15
10
5
0
G.T.
B.T.
*
*
***
**
Malate
Citrate
Isocitrate
Aconitate
2-oxoglutarate
Malonate
Nicotinic acid
Succinate
Fumarate
Quinate
Shikimate
Syringic acid
Ferulic acid
Caffeic acid
Type of carboxylate
(b)
Percent of total Aconitate
120
90
60
30
0
cis-Aconitate
trans-Aconitate
***
***
98%
2%
G.T.
B.T.
Species
(c)
Ca concentration (μmol g-1 DW)
2000
1500
1000
500
0
G.T.
B.T.
a
d
d
d
b
c
EP
PM
SM
Leaf cell type
(d)
O
Ca
Grevillea thelemanniana
Banksia telmatiaea
0
>500